Exotic Shape Systematics in $N = 136$ Region: Tracing Molecular Symmetries in Sub-Atomic Physics – Example of Actinides

Irene Dedes

The Henryk Niewodniczański
Institute of Nuclear Physics
Polish Academy of Sciences
Kraków, Poland

20 April 2023
Faculty of Physics, University of Warsaw
Warsaw, Poland

In Collaboration with:

Jerzy Dudek
IPHC and University of Strasbourg, France

Andrzej Baran, Andrzej Góźdź and Jie Yang
UMCS, Lublin, Poland

Dominique Curien and David Rouvel
IPHC and University of Strasbourg, France

Rami Gaamouci
IFJ Polish Academy of Sciences, Kraków, Poland

Mathew Martin, Kris Starosta
Simon Fraser University, Burnaby, British Columbia, Canada

Aleksandra Pędrak
National Centre for Nuclear Research, Warsaw, Poland

Hua-Lei Wang
Zhengzhou University, Zhengzhou, China

THE HENRYK NIEWODNICZAŃSKI INSTITUTE OF NUCLEAR PHYSICS POLISH ACADEMY OF SCIENCES

iPHC Institut Pluridisciplinaire Hubert CURIEN STRASBOURG

cnrs dépasser les frontières

Université de Strasbourg

Why Are We Interesed
in Molecular Symmetries
in Sub-Atomic Physics ?

Why Are We Interesed **in Molecular Symmetries** in Sub-Atomic Physics ?

• Nuclear symmetries generate unprecedented **degeneracies** in both **individual-nucleonic** and **collective-rotational levels: New Issues !**

Why Are We Interesed
in Molecular Symmetries
in Sub-Atomic Physics ?

- Nuclear symmetries generate unprecedented **degeneracies** in both **individual-nucleonic** and **collective-rotational levels: New Issues !**
- Thus – Implied totally new spectroscopy rules in subatomic physics

Why Are We Interesed in Molecular Symmetries in Sub-Atomic Physics ?

• Nuclear symmetries generate unprecedented **degeneracies** in both **individual-nucleonic** and **collective-rotational levels: New Issues !**

• Thus – Implied totally new spectroscopy rules in subatomic physics

• We found the first experimental confirmation of T_d in ^{152}Sm nucleus

Why Are We Interesed in Molecular Symmetries in Sub-Atomic Physics ?

• Nuclear symmetries generate unprecedented **degeneracies** in both **individual-nucleonic** and **collective-rotational levels: New Issues !**

• Thus – Implied totally new spectroscopy rules in subatomic physics

• We found the first experimental confirmation of T_d in ^{152}Sm nucleus

• Presence of an unprecedented class of exotic shape-isomeric states

Why Are We Interesed in Molecular Symmetries in Sub-Atomic Physics ?

• Nuclear symmetries generate unprecedented **degeneracies** in both **individual-nucleonic** and **collective-rotational levels: New Issues !**

• Thus – Implied totally new spectroscopy rules in subatomic physics

• We found the first experimental confirmation of T_d in ^{152}Sm nucleus

• Presence of an unprecedented class of exotic shape-isomeric states

FURTHER CONSEQUENCES for SUBATOMIC PHYSICS

• New highway towards exotic nuclei: Isomers living longer than G-S
• Astrophysics: New magic numbers for the nucleosynthesis

Our Interests in High-Rank Symmetries – II

• Theory predicts whole families of nuclear shapes in many regions of the Periodic Table compatible with new, exotic symmetries

• These symmetries may lead to well pronounced potential energy minima generating unprecedented, new nuclear quantum mechanisms

• For instance: unprecedented degeneracies of nucleonic levels that are neither equal to $(2j+1)$ nor to 2 (time-up, time-down ↔ KRAMERS)

• For instance: exotic (16-fold) degeneracies of 2p-2h excitations

• For instance: unprecedented degeneracies of rotational states

• For instance: unprecedented forms of the nuclear rotational behaviour - rotational bands without 'rotational E2-transitions'

• ... and many more

Our Interests in High-Rank Symmetries – II

• Theory predicts whole families of nuclear shapes in many regions of the Periodic Table compatible with new, exotic symmetries

• These symmetries may lead to well pronounced potential energy minima generating unprecedented, new nuclear quantum mechanisms

• For instance: unprecedented degeneracies of nucleonic levels that are neither equal to $(2j+1)$ nor to 2 (time-up, time-down ↔ KRAMERS)

• For instance: exotic (16-fold) degeneracies of 2p-2h excitations

• For instance: unprecedented degeneracies of rotational states

• For instance: unprecedented forms of the nuclear rotational behaviour - rotational bands without 'rotational E2-transitions'

• ... and many more

Our Interests in High-Rank Symmetries – II

- Theory predicts whole families of nuclear shapes in many regions of the Periodic Table compatible with new, exotic symmetries
- These symmetries may lead to well pronounced potential energy minima generating unprecedented, new nuclear quantum mechanisms
- For instance: unprecedented degeneracies of nucleonic levels that are neither equal to $(2j+1)$ nor to 2 (time-up, time-down ↔ KRAMERS)
- For instance: exotic (16-fold) degeneracies of 2p-2h excitations
- For instance: unprecedented degeneracies of rotational states
- For instance: unprecedented forms of the nuclear rotational behaviour - rotational bands without 'rotational E2-transitions'
- ... and many more

Our Interests in High-Rank Symmetries – II

• Theory predicts whole families of nuclear shapes in many regions of the Periodic Table compatible with new, exotic symmetries

• These symmetries may lead to well pronounced potential energy minima generating unprecedented, new nuclear quantum mechanisms

• For instance: unprecedented degeneracies of nucleonic levels that are neither equal to $(2j+1)$ nor to 2 (time-up, time-down $\leftrightarrow$ KRAMERS)

• For instance: exotic (16-fold) degeneracies of 2p-2h excitations

• For instance: unprecedented degeneracies of rotational states

• For instance: unprecedented forms of the nuclear rotational behaviour - rotational bands without 'rotational E2-transitions'

• ... and many more

Our Interests in High-Rank Symmetries – II

• Theory predicts whole families of nuclear shapes in many regions of the Periodic Table compatible with new, exotic symmetries

• These symmetries may lead to well pronounced potential energy minima generating unprecedented, new nuclear quantum mechanisms

• For instance: unprecedented degeneracies of nucleonic levels that are neither equal to $(2j+1)$ nor to 2 (time-up, time-down ↔ KRAMERS)

• For instance: exotic (16-fold) degeneracies of 2p-2h excitations

• For instance: unprecedented degeneracies of rotational states

• For instance: unprecedented forms of the nuclear rotational behaviour - rotational bands without 'rotational E2-transitions'

• ... and many more

Our Interests in High-Rank Symmetries – II

• Theory predicts whole families of nuclear shapes in many regions of the Periodic Table compatible with new, exotic symmetries

• These symmetries may lead to well pronounced potential energy minima generating unprecedented, new nuclear quantum mechanisms

• For instance: unprecedented degeneracies of nucleonic levels that are neither equal to $(2j + 1)$ nor to 2 (time-up, time-down ↔ KRAMERS)

• For instance: exotic (16-fold) degeneracies of 2p-2h excitations

• For instance: unprecedented degeneracies of rotational states

• For instance: unprecedented forms of the nuclear rotational behaviour - rotational bands without 'rotational E2-transitions'

• ... and many more

Our Interests in High-Rank Symmetries – II

• Theory predicts whole families of nuclear shapes in many regions of the Periodic Table compatible with new, exotic symmetries

• These symmetries may lead to well pronounced potential energy minima generating unprecedented, new nuclear quantum mechanisms

• For instance: unprecedented degeneracies of nucleonic levels that are neither equal to $(2j + 1)$ nor to 2 (time-up, time-down ↔ KRAMERS)

• For instance: exotic (16-fold) degeneracies of 2p-2h excitations

• For instance: unprecedented degeneracies of rotational states

• For instance: unprecedented forms of the nuclear rotational behaviour - rotational bands without ‘rotational E2-transitions’

• ... and many more

Part 1-A

Remarks about Our Choice of Theory Approach:

Phenomenological Mean Field

About Deformed Woods-Saxon Hamiltonian:
Reminding Standard Definitions

Nucleonic Density - vs. - Nuclear Potential

- The short range of the nuclear forces, comparable to the nucleon sizes, imply that the nuclear potential quickly vanishes as soon as the nucleon 'tries to escape' from the nuclear interior [vanishing density]

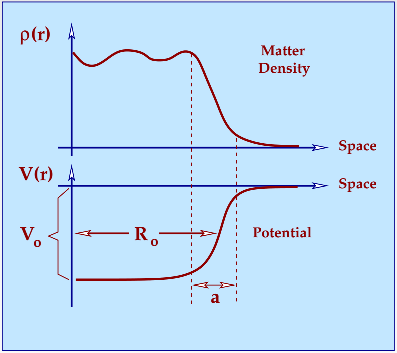

- A phenomenological [Woods-Saxon] parameterisation of the potential:

$$V(\vec{r}; V_o, R, a) = \frac{V_o}{1 + \exp[\mathrm{dist}_\Sigma(\vec{r})/a]}$$

$$V_o \approx -50\,\mathrm{MeV}, \quad a \approx 0.6\,\mathrm{fm},$$

$$R \approx 1.2\,A^{1/3}\,\mathrm{fm}$$

- Function $\mathbf{dist}_\Sigma(\vec{r})$ gives the shortest distance between the nuclear surface and a point in space (see next slides)

- Among ~3 000 nuclei known today, the great majority are deformed (~8 spherical)

Description of Nuclear Deformation [or Shapes]

• Given nuclear surface, Σ. It can generally be expanded in terms of the spherical harmonic basis $\{Y_{\lambda\mu}(\vartheta,\varphi)\}$

Given surface Σ

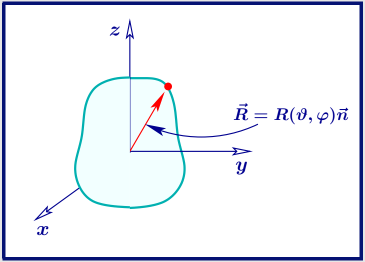

$\vec{n} = \{\cos\varphi \sin\vartheta, \sin\varphi \sin\vartheta, \cos\vartheta\}$

The lowest rank deformations:

→ $\alpha_{2\mu}$ - quadrupole
→ $\alpha_{3\mu}$ - octupole
→ $\alpha_{4\mu}$ - hexadecapole

• The formal expansion [standard form]:

$$R(\vartheta,\varphi) = R_o\, c(\{\alpha\}) \left[1+\sum_{\lambda\mu} \alpha_{\lambda\mu} Y_{\lambda\mu}(\vartheta,\varphi)\right]$$

= a multipole expansion about the sphere

• Parameters $\{\alpha_{\lambda\mu}\}$, are called *deformations* or shape degrees of freedom

• In the case of time-dependent description e.g., collective vibrations and/or rotations:

$$\boxed{\alpha_{\lambda\mu} = \alpha_{\lambda\mu}(t)}$$

WS Mean-Field is a Functional of $\mathrm{dist}_\Sigma(\vec{r})$

Surface Σ : $R(\vartheta,\varphi) = R_o\, c(\{\alpha\}) \left[1 + \sum_{\lambda\mu} \alpha_{\lambda\mu} Y_{\lambda\mu}(\vartheta,\varphi)\right]$

Given surface $\Sigma \Leftrightarrow \mathrm{dist}_\Sigma(\vec{r})$

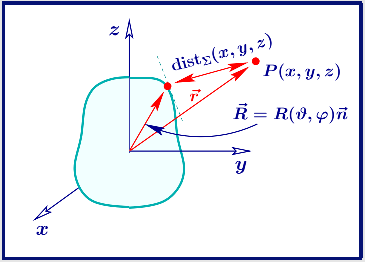

$\vec{n} = \{\cos\varphi \sin\vartheta, \sin\varphi\sin\vartheta, \cos\vartheta\}$

- WS Potential respects automatically the surface-Σ symmetries:

$$V(\vec{r}; V_o, R, a) = \frac{V_o}{1+\exp[\mathrm{dist}_\Sigma(\vec{r})/a]}$$

- Auxiliary function

$$f(\vartheta,\varphi) \equiv \left[\vec{r} - R(\vartheta,\varphi)\,\vec{n}(\vartheta,\varphi)\right]^2$$

- Distance function

$$\mathrm{dist}_\Sigma(\vec{r}) \equiv \min_{\{\vartheta,\varphi\}} f(\vartheta,\varphi)$$

Mean-Field Potential: $\hat{\mathcal{V}}_{\mathrm{m-f}} = \hat{\mathcal{V}}^{\mathrm{WS}}_{\mathrm{cent}} + \hat{\mathcal{V}}^{\mathrm{WS}}_{\mathrm{SO}} + \hat{\mathcal{V}}_{\mathrm{C}}$

Hamiltonian: $\hat{\mathcal{H}}_{\mathrm{m-f}} = \hat{\mathcal{T}} + \hat{\mathcal{V}}_{\mathrm{m-f}}$

Introducing Woods-Saxon Hamiltonian

- We use the phenomenological **Woods-Saxon Hamiltonian** with the so-called **'universal'** parameterisation

⇒ fixed set of parameters for thousands of nuclei!

- **Central Potential**

$$\mathcal{V}_{\text{cent}}^{\text{WS}} = \frac{V_c}{1 + \exp\left[\text{dist}_\Sigma(\vec{r}; r_c)/a_c\right]}$$

- **Spin-Orbit Potential**

$$\mathcal{V}_{\text{SO}}^{\text{WS}} = \frac{2\hbar\,\lambda_{so}}{(2mc)^2}[(\vec{\nabla}V_{\text{SO}}^{\text{WS}}) \wedge \hat{p}\,] \cdot \hat{s}, \;\text{ with } V_{\text{SO}}^{\text{WS}} = \frac{V_o}{1 + \exp[\text{dist}_\Sigma(\vec{r}, r_{so})/a_{so}]}$$

- **Isospin distinction** (+ ↔ protons) and (− ↔ neutrons)

$$V_c = V_o\left[1 \pm \kappa_c \frac{N-Z}{N+Z}\right]; \quad \lambda_{so} = \lambda_o\left[1 \pm \kappa_{so}\frac{N-Z}{N+Z}\right]$$

- **This potential depends *only* on two sets of 6 parameters ↔ Mass Table**

$$\boxed{\{V_c, r_c, a_c; \lambda_{so}, r_{so}, a_{so}\}_{\pi,\nu}} \Leftrightarrow \boxed{\{V_o, \kappa_c, r_c^{\pi,\nu}, a_c^{\pi,\nu}; \lambda_o, \kappa_{so}, r_{so}^{\pi,\nu}, a_{so}^{\pi,\nu}\}}$$

About Choices between Mean-Field Approaches

• Our group was investing in phenomenological Woods-Saxon (WS) and microscopic Skyrme Hartree-Fock-Bogolyubov (HFB) approaches

• For this project we select the phenomenological WS-type description

• This will allow us to profit from our earlier applications of inverse problem theory – and resulting stabilisation of modelling-predictions*)

---

*) Dudek, Szpak, Porquet, Molique, Rybak and Fornal,
J. Phys. G: Nucl. Part. Phys. **37** (2010) 064031

*) Dudek, Rybak, Szpak, Porquet, Molique and Fornal,
Int. J. Mod. Phys. E**19** (2010) 652

*) Dedes and Dudek,
Act. Phys. Pol. B Proc. Supp., Vol. **10**, No. 1 (2017)

*) Dedes and Dudek,
Physica Scripta, Vol.**93**, No. 4 (2018)

*) Dedes and Dudek,
Physical Review C **99** (2019) 054310

*) *“Stochastic approach to the problem of predictive power in the theoretical modelling of the nuclear mean-field”*,
I. Dedes, PhD Thesis (2017), `http://www.theses.fr/2017STRAE017/document`

Part 1-B

Our Approach to Hamiltonian Optimisation

Inverse Problem Theory
and
Monte-Carlo Simulations

“Predictive Power of Our Hamiltonian”

What Does It Mean To Predict?

What Does It Mean To Predict?

- Any calculation performed with any given model (theory) before experimental result is known can be called *a prediction*

What Does It Mean To Predict?

• Any calculation performed with any given model (theory) before experimental result is known can be called *a prediction*

• Only after experimental verification we can declare that the prediction was *good* or *poor*

What Does It Mean To Predict?

• Any calculation performed with any given model (theory) before experimental result is known can be called *a prediction*

• Only after experimental verification we can declare that the prediction was *good* or *poor*

• *A prediction* has always *a predictive power*. However:

What does it mean to have *good* predictive power?

What are the criteria of the quality of the prediction?

What Does It Mean To Predict?

• Any calculation performed with any given model (theory) before experimental result is known can be called *a prediction*

• Only after experimental verification we can declare that the prediction was *good* or *poor*

• *A prediction* has always *a predictive power*. However:

What does it mean to have *good* predictive power?

What are the criteria of the quality of the prediction?

• Introducing quality criteria, we introduce *a subjective judgment*, since being good for someone may not be even satisfactory for someone else

What Does It Mean To Predict?

• Any calculation performed with any given model (theory) before experimental result is known can be called *a prediction*

• Only after experimental verification we can declare that the prediction was *good* or *poor*

• *A prediction* has always *a predictive power*. However:

What does it mean to have *good* predictive power?

What are the criteria of the quality of the prediction?

• Introducing quality criteria, we introduce *a subjective judgment*, since being good for someone may not be even satisfactory for someone else

⇒ Conclusion:

One needs to introduce a framework which will help to compare the model prediction capacities

Predictive Power of Theories: Stochastic Approach

This part of our research project is formulated within

Stochastic Theory of Predictive Power[*)]

[*)] **Introduced in "Open Problems in Nuclear Theory", J. Dudek and collaborators, J. Phys. G: Nucl. Part. Phys. 37 (2010) 064031**

Predictive Power of Theories: Stochastic Approach

This part of our research project is formulated within

Stochastic Theory of Predictive Power[*)]

- Given theory $\mathcal{T}$, of a quantum phenomenon $\mathcal{P}$, employing observables $\rightarrow$

Operators : $\hat{\mathcal{F}}_1, \hat{\mathcal{F}}_2, \ldots \hat{\mathcal{F}}_p$

[*)] **Introduced in "Open Problems in Nuclear Theory", J. Dudek and collaborators, J. Phys. G: Nucl. Part. Phys. 37 (2010) 064031**

Predictive Power of Theories: Stochastic Approach

This part of our research project is formulated within

Stochastic Theory of Predictive Power*)

- Given theory $\mathcal{T}$, of a quantum phenomenon $\mathcal{P}$, employing observables $\rightarrow$

  Operators : $\hat{\mathcal{F}}_1, \hat{\mathcal{F}}_2, \ldots \hat{\mathcal{F}}_p$

- Observables will be characterised not only by related eigenvalues i.e. $\{f_j\}$

$$\left[\hat{\mathcal{F}}_1 \rightarrow \{f_1\}, \quad \hat{\mathcal{F}}_2 \rightarrow \{f_2\}, \quad \ldots \; \hat{\mathcal{F}}_p \rightarrow \{f_p\}\right]$$

*) Introduced in "Open Problems in Nuclear Theory", J. Dudek and collaborators, J. Phys. G: Nucl. Part. Phys. 37 (2010) 064031

Predictive Power of Theories: Stochastic Approach

This part of our research project is formulated within

Stochastic Theory of Predictive Power*)

- Given theory $\mathcal{T}$, of a quantum phenomenon $\mathcal{P}$, employing observables $\rightarrow$

  Operators : $\hat{\mathcal{F}}_1, \hat{\mathcal{F}}_2, \ldots \hat{\mathcal{F}}_p$

- Observables will be characterised not only by related eigenvalues i.e. $\{f_j\}$

  $$\big[\hat{\mathcal{F}}_1 \rightarrow \{f_1\}, \quad \hat{\mathcal{F}}_2 \rightarrow \{f_2\}, \quad \ldots \; \hat{\mathcal{F}}_p \rightarrow \{f_p\}\big]$$

  but also by distributions of probability of their validity - or applicability

  $$\mathcal{P}_1 = \mathcal{P}_1(f_1), \;\; \mathcal{P}_2 = \mathcal{P}_2(f_2), \; \ldots \; \mathcal{P}_p = \mathcal{P}_1(f_p)$$

*) **Introduced in "Open Problems in Nuclear Theory", J. Dudek and collaborators, J. Phys. G: Nucl. Part. Phys. 37 (2010) 064031**

Predictive Power of Theories: Stochastic Approach

This part of our research project is formulated within

Stochastic Theory of Predictive Power*)

- Given theory $\mathcal{T}$, of a quantum phenomenon $\mathcal{P}$, employing observables $\to$

  Operators : $\hat{\mathcal{F}}_1, \hat{\mathcal{F}}_2, \ldots \hat{\mathcal{F}}_p$

- Observables will be characterised not only by related eigenvalues i.e. $\{f_j\}$

$$\left[\hat{\mathcal{F}}_1 \to \{f_1\}, \quad \hat{\mathcal{F}}_2 \to \{f_2\}, \quad \ldots\ \hat{\mathcal{F}}_p \to \{f_p\}\right]$$

  but also by distributions of probability of their validity - or applicability

$$\mathcal{P}_1 = \mathcal{P}_1(f_1), \;\; \mathcal{P}_2 = \mathcal{P}_2(f_2), \;\ldots\; \mathcal{P}_p = \mathcal{P}_1(f_p)$$

- These distributions are obtained using stochastic methods on the basis of **all the uncertainties known-, or possible to estimate today**

*) **Introduced in "Open Problems in Nuclear Theory", J. Dudek and collaborators, J. Phys. G: Nucl. Part. Phys. 37 (2010) 064031**

Direct and Inverse Problems in Quantum Theories

- Given parameters $\{p\} \longrightarrow$ The Schrödinger equation produces 'data':

$$\hat{H}(p)\psi = E_p\psi \rightarrow \{E_p, \psi(p)\} \leftrightarrow \boxed{\hat{O}_H(p) = d^{th} \leftarrow \textit{Direct Problem}}$$

Direct and Inverse Problems in Quantum Theories

- Given parameters $\{p\}$ $\longrightarrow$ The Schrödinger equation produces 'data':

$$\hat{H}(p)\psi = E_p\psi \to \{E_p, \psi(p)\} \leftrightarrow \boxed{\hat{O}_H(p) = d^{th} \leftarrow \textit{Direct Problem}}$$

- To find the optimal parameters we must invert the above relation:

$$\boxed{p^{opt} = \hat{O}_H^{-1}(d^{exp}) \leftarrow \textit{Inverse Problem}}$$

Direct and Inverse Problems in Quantum Theories

• Given parameters $\{p\} \longrightarrow$ The Schrödinger equation produces 'data':

$$\hat{H}(p)\psi = E_p\psi \rightarrow \{E_p, \psi(p)\} \leftrightarrow \boxed{\hat{O}_H(p) = d^{th} \leftarrow \textit{Direct Problem}}$$

• To find the optimal parameters we must invert the above relation:

$$\boxed{p^{opt} = \hat{O}_H^{-1}(d^{exp}) \leftarrow \textit{Inverse Problem}}$$

• In many-body theories the existence of operator $\hat{O}_{\mathbf{H}}^{-1}$ is doubtful, in fact no mathematical methods of such a construction are known

Direct and Inverse Problems in Quantum Theories

- Given parameters $\{p\}$ $\longrightarrow$ The Schrödinger equation produces 'data':

$$\hat{H}(p)\psi = E_p\psi \rightarrow \{E_p, \psi(p)\} \leftrightarrow \boxed{\hat{O}_H(p) = d^{th} \leftarrow \textit{Direct Problem}}$$

- To find the optimal parameters we must invert the above relation:

$$\boxed{p^{opt} = \hat{O}_H^{-1}(d^{exp}) \leftarrow \textit{Inverse Problem}}$$

- In many-body theories the existence of operator $\hat{O}_{\mathbf{H}}^{-1}$ is doubtful, in fact no mathematical methods of such a construction are known

If $\hat{O}_{\mathbf{H}}$ has no inverse we say that inverse problem is ill-posed

Direct and Inverse Problems in Quantum Theories

- Given parameters $\{p\} \to$ The Schrödinger equation produces 'data':

$$\hat{H}(p)\psi = E_p\psi \to \{E_p, \psi(p)\} \leftrightarrow \boxed{\hat{O}_H(p) = d^{th} \leftarrow \textit{Direct Problem}}$$

- To find the optimal parameters we must invert the above relation:

$$\boxed{p^{opt} = \hat{O}_H^{-1}(d^{exp}) \leftarrow \textit{Inverse Problem}}$$

- In many-body theories the existence of operator $\hat{O}_{\mathbf{H}}^{-1}$ is doubtful, in fact no mathematical methods of such a construction are known

If $\hat{O}_{\mathbf{H}}$ has no inverse we say that inverse problem is ill-posed

In many-body Hamiltonian case this issue remains unsolved:
Instead of solving the Inverse Problem → "**one minimises χ^2**"

Inverse Problem in Linearised Representation

- Definition of χ^2 in the present context

$$\chi^2(p) = \sum_{j=1}^{n_d} [e_j^{\text{exp}} - e_j^{\text{th}}(p)]^2$$

$\downarrow$ Taylor linearisation

$$\frac{\partial \chi^2}{\partial p_i} = 0 \;\; \rightarrow \;\; (J^T J) \cdot p = J^T b \;\; \leftrightarrow \;\; J^T J \overset{df}{=} \mathcal{A}, \;\; \left[J_{jk} = \left(\frac{\partial e_j^{\text{th}}}{\partial p_k} \right) \right]$$

J being Jacobian matrix

Inverse Problem in Linearised Representation

- Definition of χ^2 in the present context

$$\chi^2(p) = \sum_{j=1}^{n_d} [e_j^{\text{exp}} - e_j^{\text{th}}(p)]^2$$

↓ Taylor linearisation

$$\frac{\partial \chi^2}{\partial p_i} = 0 \;\; \rightarrow \;\; (J^T J) \cdot p = J^T b \;\; \leftrightarrow \;\; J^T J \stackrel{df}{=} \mathcal{A}, \;\; \left[J_{jk} = \left(\frac{\partial e_j^{\text{th}}}{\partial p_k} \right) \right]$$

J being Jacobian matrix

- *Applied Mathematics*: From the Data $\mathcal{D}$, we extract information about the optimal parameters $\mathcal{P}$, by inverting matrix $\mathcal{A}$:

Direct Problem: $\mathcal{A} \cdot \mathcal{P} = \mathcal{D}$ $\rightarrow$ Inverse Problem: $\mathcal{P} = \mathcal{A}^{-1} \cdot \mathcal{D}$

Inverse Problem in Linearised Representation

- Definition of χ^2 in the present context

$$\chi^2(p) = \sum_{j=1}^{n_d}[e_j^{\text{exp}} - e_j^{\text{th}}(p)]^2$$

$\downarrow$ Taylor linearisation

$$\frac{\partial \chi^2}{\partial p_i} = 0 \;\; \rightarrow \;\; (J^T J) \cdot p = J^T b \;\; \leftrightarrow \;\; J^T J \overset{df}{=} \mathcal{A}, \;\; \left[J_{jk} = \left(\frac{\partial e_j^{\text{th}}}{\partial p_k}\right)\right]$$

J being Jacobian matrix

- *Applied Mathematics*: From the Data $\mathcal{D}$, we extract information about the optimal parameters $\mathcal{P}$, by inverting matrix $\mathcal{A}$:

Direct Problem: $\mathcal{A} \cdot \mathcal{P} = \mathcal{D}$ $\rightarrow$ Inverse Problem: $\mathcal{P} = \mathcal{A}^{-1} \cdot \mathcal{D}$

- In the presence of parametric correlations, say $p_k = f(p_{k'})$, two columns of $\mathcal{A}$ are linearly dependent

Inverse Problem in Linearised Representation

- Definition of χ^2 in the present context

$$\chi^2(p) = \sum_{j=1}^{n_d}[e_j^{\text{exp}} - e_j^{\text{th}}(p)]^2$$

$\downarrow$ Taylor linearisation

$$\frac{\partial\chi^2}{\partial p_i} = 0 \;\rightarrow\; (J^T J)\cdot p = J^T b \;\leftrightarrow\; J^T J \overset{df}{=} \mathcal{A}, \;\left[J_{jk} = \left(\frac{\partial e_j^{\text{th}}}{\partial p_k}\right)\right]$$

J being Jacobian matrix

- *Applied Mathematics*: From the Data $\mathcal{D}$, we extract information about the optimal parameters $\mathcal{P}$, by inverting matrix $\mathcal{A}$:

Direct Problem: $\mathcal{A}\cdot\mathcal{P} = \mathcal{D}$ $\;\rightarrow\;$ Inverse Problem: $\mathcal{P} = \mathcal{A}^{-1}\cdot\mathcal{D}$

- In the presence of parametric correlations, say $p_k = f(p_{k'})$, two columns of $\mathcal{A}$ are linearly dependent

- If this happens $\rightarrow$ $\mathcal{A}$-matrix becomes singular [Ill-Posed Problem]

Ill-Posed: Correlation between parameters and the data is lost!

Sources of Uncertainties in Theoretical Predictions

We have different uncertainty sources to take into account when parameter adjusting and predicting

Sources of Uncertainties in Theoretical Predictions

We have different uncertainty sources to take into account when parameter adjusting and predicting

1. **Experimental Errors**

Sources of Uncertainties in Theoretical Predictions

We have different uncertainty sources to take into account when parameter adjusting and predicting

1. **Experimental Errors**
2. **Parametric Correlations**

Sources of Uncertainties in Theoretical Predictions

We have different uncertainty sources to take into account when parameter adjusting and predicting

1. **Experimental Errors**
2. **Parametric Correlations**
3. **Incomplete Theories**

Sources of Uncertainties in Theoretical Predictions

We have different uncertainty sources to take into account when parameter adjusting and predicting

1. **Experimental Errors**
2. **Parametric Correlations**
3. **Incomplete Theories**

Model parameters are not just numbers!

Sources of Uncertainties in Theoretical Predictions

We have different uncertainty sources to take into account when parameter adjusting and predicting

1. **Experimental Errors**
2. **Parametric Correlations**
3. **Incomplete Theories**

Model parameters are not just numbers!

They are represented by probability uncertainty distributions

Linear Parametric Correlations
and
Pearson Correlation Matrix

Pearson Correlation Matrix $\{r_{ij}\}$

- The Pearson Correlation matrix informs us about the possible linear dependence existing between two parameters, p_i and p_j:

- Definition

$$r_{ij} = \frac{\sum_{k=1}^{n} (p_{i,k} - \bar{p}_i)(p_{j,k} - \bar{p}_j)}{\sqrt{\sum_{k=1}^{n} (p_{i,k} - \bar{p}_i)^2} \sqrt{\sum_{k=1}^{n} (p_{j,k} - \bar{p}_j)^2}}$$

where

- $k = 1, \ldots n$, with n is the number of elements for each p_i and p_j
- $\bar{p}_i = \frac{1}{n} \sum_{k=1}^{n} p_{i,k}$ is the arithmetic mean value

- Coefficient range: $r_{ij} \in [-1, +1]$

Parametric Correlations, General Illustrations

- From *Wikipedia*: two-dimensional (x, y) distributions of data-points with their corresponding values of Pearson Coefficient r_{ij}.

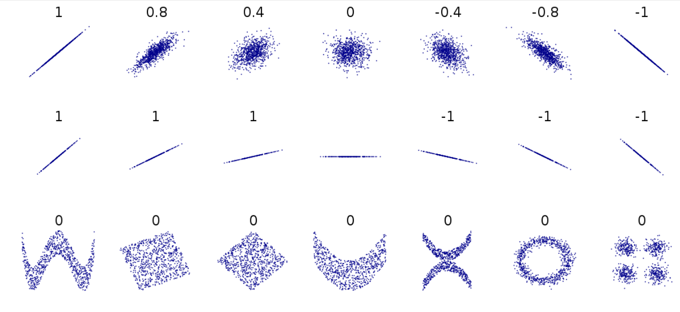

- **Observation**: The bottom row results show strongly non-linear **correlated distributions which give $r_{ij} \approx 0$**

Parametric Correlations: Monte Carlo Approach

- **Parametric correlations can be studied using Monte Carlo Simulations**

Parametric Correlations: Monte Carlo Approach

- **Parametric correlations can be studied using Monte Carlo Simulations**
  - Given space of data $\{d_1, d_2, \ldots\ d_n\}$ with uncertainties, $d \pm \sigma$
    $\{\sigma_1, \sigma_2, \ldots\ \sigma_n\}$

Parametric Correlations: Monte Carlo Approach

- **Parametric correlations can be studied using Monte Carlo Simulations**
  - Given space of data $\{d_1, d_2, \ldots\ d_n\}$ with uncertainties, $d \pm \sigma$
    $\{\sigma_1, \sigma_2, \ldots\ \sigma_n\}$
  - With a random-number generator we define what is called 'Gaussian noise distribution' around each $\{d_i\}_j$

Parametric Correlations: Monte Carlo Approach

- **Parametric correlations can be studied using Monte Carlo Simulations**
  - Given space of data $\{d_1, d_2, \ldots\ d_{\rm n}\}$ with uncertainties, $d \pm \sigma$
    $\{\sigma_1, \sigma_2, \ldots\ \sigma_{\rm n}\}$
  - With a random-number generator we define what is called 'Gaussian noise distribution' around each $\{d_i\}_j$
  - We fit the parameter sets $\{p_1, p_2, \ldots\ p_m\}_j$ great number of times, $\mathcal{N}_{MC} \sim 10^5$, i.e. for $j = 1, 2, \ \ldots\ \mathcal{N}_{MC}$

Parametric Correlations: Monte Carlo Approach

- **Parametric correlations can be studied using Monte Carlo Simulations**
  - Given space of data $\{d_1, d_2, \ldots\ d_\mathrm{n}\}$ with uncertainties, $d \pm \sigma$
    $\{\sigma_1, \sigma_2, \ldots\ \sigma_\mathrm{n}\}$
  - With a random-number generator we define what is called 'Gaussian noise distribution' around each $\{d_i\}_j$
  - We fit the parameter sets $\{p_1, p_2, \ldots\ p_m\}_j$ great number of times, $\mathcal{N}_{MC} \sim 10^5$, i.e. for $j = 1, 2, \ \ldots\ \mathcal{N}_{MC}$
  - From m-tuplets of obtained parameters, $\{p_1, p_2, \ldots\ p_m\}$, we construct the tables and projection plots

Parametric Correlations: Monte Carlo Approach

- **Parametric correlations can be studied using Monte Carlo Simulations**
  - Given space of data $\{d_1, d_2, \ldots\ d_\mathrm{n}\}$ with uncertainties, $d \pm \sigma$
    $\{\sigma_1, \sigma_2, \ldots\ \sigma_\mathrm{n}\}$
  - With a random-number generator we define what is called 'Gaussian noise distribution' around each $\{d_i\}_j$
  - We fit the parameter sets $\{p_1, p_2, \ldots\ p_m\}_j$ great number of times, $\mathcal{N}_{MC} \sim 10^5$, i.e. for $j = 1, 2, \ \ldots\ \mathcal{N}_{MC}$
  - From m-tuplets of obtained parameters, $\{p_1, p_2, \ldots\ p_m\}$, we construct the tables and projection plots
  - For each m-tuplet, we can calculate the single particle energies for different nuclei and construct the occurrence histograms for each energy state

Parametric Correlations: Monte Carlo Approach

- **Parametric correlations can be studied using Monte Carlo Simulations**
  - Given space of data $\{d_1, d_2, \ldots\ d_\mathrm{n}\}$ with uncertainties, $d \pm \sigma$
    $\{\sigma_1, \sigma_2, \ldots\ \sigma_\mathrm{n}\}$
  - With a random-number generator we define what is called 'Gaussian noise distribution' around each $\{d_i\}_j$
  - We fit the parameter sets $\{p_1, p_2, \ldots\ p_m\}_j$ great number of times, $\mathcal{N}_{MC} \sim 10^5$, i.e. for $j = 1, 2, \ \ldots\ \mathcal{N}_{MC}$
  - From m-tuplets of obtained parameters, $\{p_1, p_2, \ldots\ p_m\}$, we construct the tables and projection plots
  - For each m-tuplet, we can calculate the single particle energies for different nuclei and construct the occurrence histograms for each energy state

- **We consider the single particle energies of the 'experimentally known' doubly-magic spherical-nuclei as the space of data $\{d_i\}_j$:**

$$^{16}_{8}\mathrm{O}_{8},\ ^{40}_{20}\mathrm{Ca}_{20},\ ^{48}_{20}\mathrm{Ca}_{28},\ ^{56}_{28}\mathrm{Ni}_{28},\ ^{90}_{40}\mathrm{Zr}_{50},\ ^{132}_{50}\mathrm{Sn}_{82},\ ^{146}_{64}\mathrm{Gd}_{82},\ ^{208}_{82}\mathrm{Pb}_{126}$$

Parametric Correlations in WS Hamiltonian

- Reminder about WS-parameters: $\{V_o, \kappa_c, r_c^{\pi,\nu}, a_c^{\pi,\nu}; \lambda_o, \kappa_{so}, r_{so}^{\pi,\nu}, a_{so}^{\pi,\nu}\}$

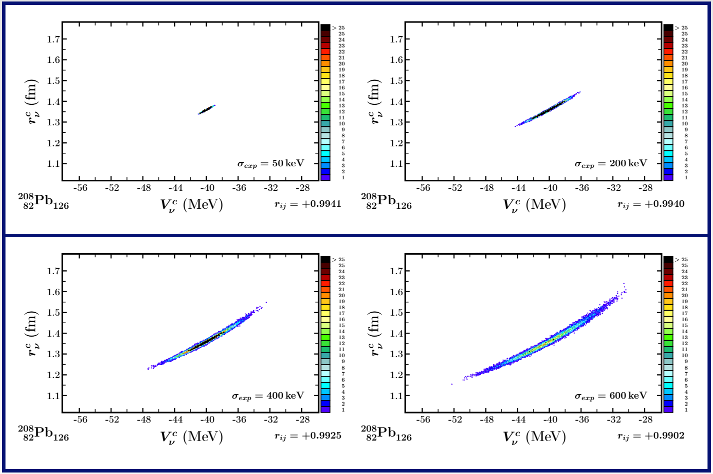

- These results show that the central potential depth and central potential radius parameters are correlated. We have ($r_{ij} \approx 1$). We show that: $V_c \times r_c^2 \approx \text{const.}$

Parametric Correlations in WS Hamiltonian

- Reminder about WS-parameters: $\{V_o, \kappa_c, r_c^{\pi,\nu}, a_c^{\pi,\nu}; \lambda_o, \kappa_{so}, r_{so}^{\pi,\nu}, a_{so}^{\pi,\nu}\}$

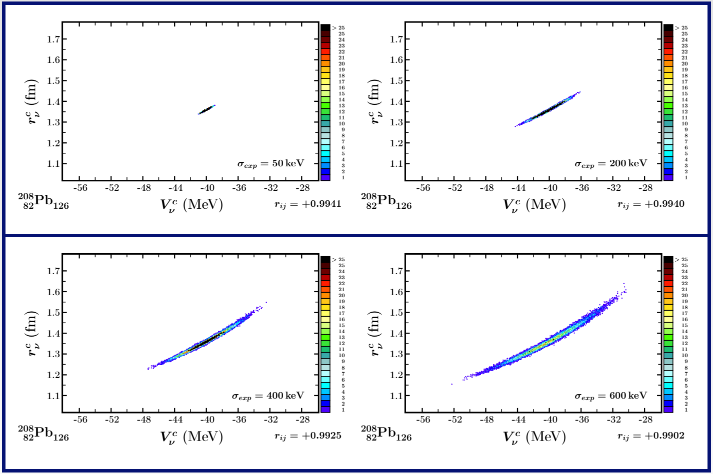

- These results show that the central potential depth and central potential radius parameters are correlated. We have ($r_{ij} \approx 1$). We show that: $V_c \times r_c^2 \approx$ const.
- Parameters V_0^c *vs.* r_π^c show approximately parabolic correlation

Parametric Correlation Analysis: Observations

Central Potential Parameters

• Our analysis shows a quadratic ('parabolic') dependence between central depth and central radius

• We may fit the expression $r_c = \alpha \cdot V_c^2 + \beta \cdot V_c + \gamma$

Parametric Correlations in WS Hamiltonian

- Reminder about WS-parameters: $\{V_o, \kappa_c, r_c^{\pi,\nu}, a_c^{\pi,\nu}; \lambda_o, \kappa_{so}, r_{so}^{\pi,\nu}, a_{so}^{\pi,\nu}\}$

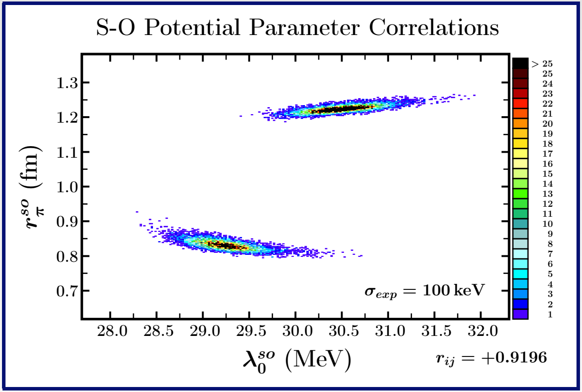

Parametric Correlations in WS Hamiltonian

- Reminder about WS-parameters: $\{V_o, \kappa_c, r_c^{\pi,\nu}, a_c^{\pi,\nu}; \lambda_o, \kappa_{so}, r_{so}^{\pi,\nu}, a_{so}^{\pi,\nu}\}$

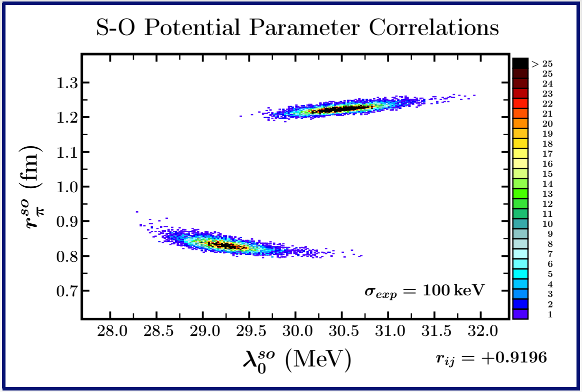

- Parameters λ_0^{so} *vs.* r_π^{so}:

present ‘double valued approximate linear correlations’

We call them **compact** and **non-compact** spin-orbit radius parametrisations

Parametric Correlation Analysis: Observations

Spin-Orbit Potential Parameters

• For spin-orbit parameters we have 'double-bubble' structure → i.e.: no "usual" function of the type $y = f(x)$ can be defined

• Since we can clearly separate the distributions leading to the "double bubbles', we select two separate solutions corresponding to the two maxima of distributions. The results are given in the Table:

Type/name	r_ν^{so} [fm]	r_π^{so} [fm]
compact	0.89	0.83
non-compact	1.19	1.22

Parametric Correlation Elimination

Before Parametric Correlation Elimination:

12 independent parameters

$$\{V_o, \kappa_c, r_c^{\pi,\nu}, a_c^{\pi,\nu}; \lambda_o, \kappa_{so}, r_{so}^{\pi,\nu}, a_{so}^{\pi,\nu}\}$$

After Parametric Correlation Elimination:

6 independent parameters

$$\{V_o, \kappa_c, a_c^{\pi,\nu}; \lambda_o, \kappa_{so}\}$$

New Universal WS Hamiltonian Parametrisation

- We chose the compact solution since it gives better comparison with experiment as compared to the non-compact one

	V_0^c (MeV)	κ^c	$a^c_{\pi,\nu}$ (fm)	λ_0^{so}	κ^{so}
Mean values	−50.225	0.624	0.594 (π) 0.572 (ν)	26.210	−0.683
Standard error	0.142	0.013	0.010 (π) 0.011 (ν)	0.513	0.139

- The resulting dependent parameters are

$$r^c_\pi = 1.278\,\text{fm},\; r^c_\nu = 1.265\,\text{fm},$$

and

$$r^{so}_\pi = 0.830\,\text{fm},\; r^{so}_\nu = 0.890\,\text{fm}.$$

- The spin-orbit diffusivity parameters, $a^{so}_\pi = a^{so}_\nu = 0.700\,\text{fm}$.

Final Comparison: Compact Solution – Neutrons

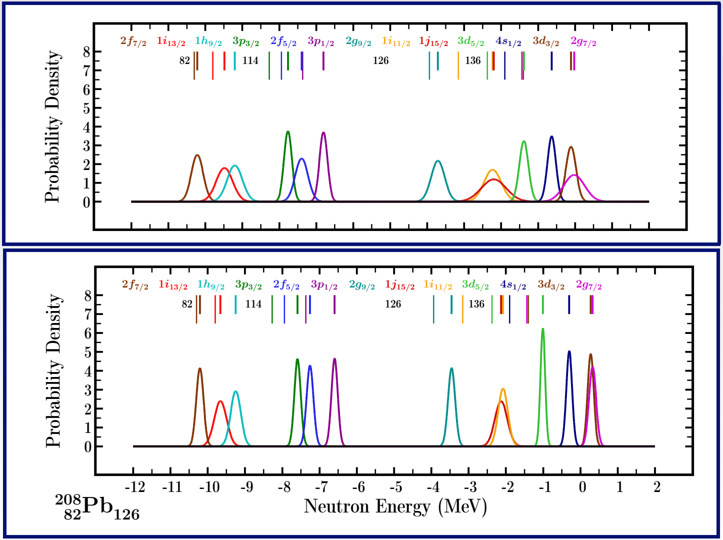

- **Top**: Full parametric freedom, **Bottom:** Full parametric correlation elimination
- Please observe significantly narrower peaks after parametric correlation removal

Final Comparison: Compact Solution – Protons

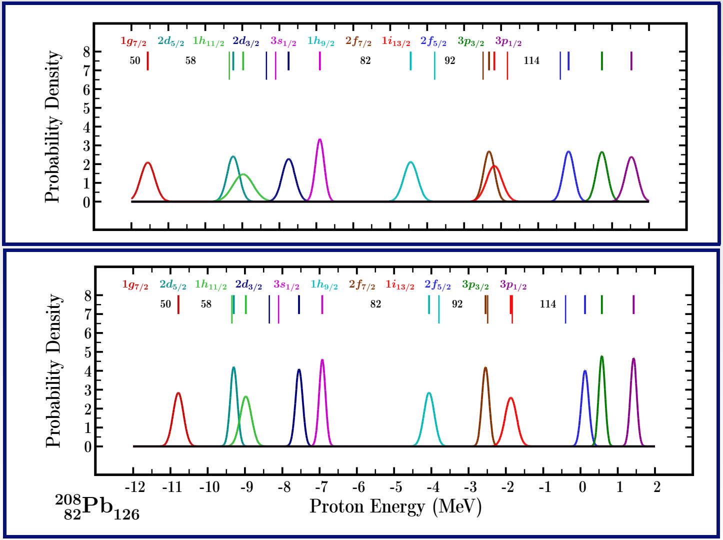

- **Top**: Full parametric freedom, **Bottom:** Full parametric correlation elimination
- Please observe significantly narrower peaks after parametric correlation removal

Part 2

Selected Molecular Symmetries in Atomic Nuclei

Example: So-called High-Rank*) Symmetries Tetrahedral T_d and Octahedral O_h

*) The only ones with 4D irreducible spinor representations – 4-fold nucleonic degeneracies

Tetrahedral Symmetry: Spherical-Harmonic Basis

Only special combinations of spherical harmonics may form a basis for surfaces with tetrahedral symmetry and only odd-order except 5

Three Lowest Order Solutions: Rank ↔ Multipolarity λ

$$\lambda = 3: \quad t_1 \equiv \alpha_{3,\pm 2}$$

$\lambda = 5:$ no solution possible

$$\lambda = 7: \quad t_2 \equiv \alpha_{7,\pm 2} \quad \text{and} \quad \alpha_{7,\pm 6} = -\sqrt{\tfrac{11}{13}} \cdot \alpha_{7,\pm 2}$$

$$\lambda = 9: \quad t_3 \equiv \alpha_{9,\pm 2} \quad \text{and} \quad \alpha_{9,\pm 6} = +\sqrt{\tfrac{28}{198}} \cdot \alpha_{9,\pm 2}$$

$$R(\vartheta,\varphi) = R_o\, c(\{\alpha\}) \left[1 + \textstyle\sum_{\lambda\mu} \alpha_{\lambda\mu} Y_{\lambda\mu}(\vartheta,\varphi)\right]$$

- Problem presented in detail in:

J. Dudek, J. Dobaczewski, N. Dubray, A. Góźdź, V. Pangon and N. Schunck, Int. J. Mod. Phys. E16, 516 (2007) [516-532].

Nuclear Tetrahedral Shapes – 3D Examples

Illustrations below show the tetrahedral-symmetric surfaces at three increasing values of rank $\lambda = 3$ deformations α_{32}: 0.1, 0.2 and 0.3

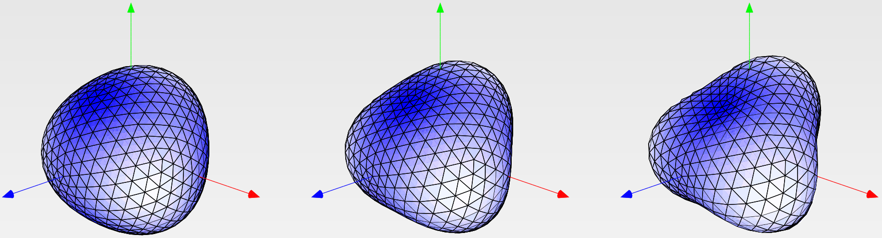

$\alpha_{32} \equiv t_1 = 0.1$ $\alpha_{32} \equiv t_1 = 0.2$ $\alpha_{32} \equiv t_1 = 0.3$

Observations:

- There are infinitely many tetrahedral-symmetric surfaces
- Nuclear 'pyramids' do not resemble pyramids very much!

OBSERVATION:

Tetrahedral symmetry group, T_d,
is a sub-group of the octahedral one, O_h

Octahedral Symmetry: Spherical-Harmonic Basis

Only special combinations of spherical harmonics may form a basis for surfaces with octahedral symmetry and only in even-orders $\lambda \geq 4$

Three Lowest Order Solutions: Rank $\leftrightarrow$ Multipolarity λ

$$\lambda = 4: \quad o_1 \equiv \quad \alpha_{40} \quad \text{and} \quad \alpha_{4,\pm 4} = -\sqrt{\tfrac{5}{14}} \cdot \alpha_{40}$$

$$\lambda = 6: \quad o_2 \equiv \quad \alpha_{60} \quad \text{and} \quad \alpha_{6,\pm 4} = -\sqrt{\tfrac{7}{2}} \cdot \alpha_{60}$$

$$\lambda = 8: \quad o_3 \equiv \quad \alpha_{80} \quad \text{and} \quad \alpha_{8,\pm 4} = \sqrt{\tfrac{28}{198}} \cdot \alpha_{80}$$

$$\text{and} \quad \alpha_{8,\pm 8} = \sqrt{\tfrac{65}{198}} \cdot \alpha_{80}$$

$$R(\vartheta, \varphi) = R_o\, c(\{\alpha\}) \left[1 + \sum_{\lambda\mu} \alpha_{\lambda\mu} Y_{\lambda\mu}(\vartheta, \varphi)\right]$$

- Problem presented in detail in:

J. Dudek, J. Dobaczewski, N. Dubray, A. Góźdź, V. Pangon and N. Schunck, Int. J. Mod. Phys. E16, 516 (2007) [516-532].

Nuclear Octahedral Shapes – 3D Examples

Illustrations below show the octahedral-symmetric surfaces at three increasing values of rank $\lambda = 4$ deformations o_4: 0.1, 0.2 and 0.3

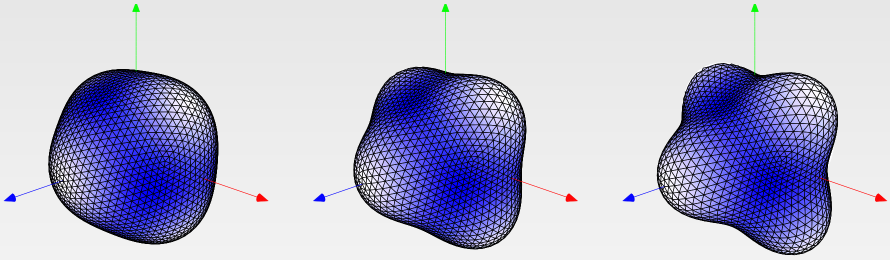

$o_1 = 0.1$ $o_1 = 0.2$ $o_1 = 0.3$

Observations:

- There are infinitely many octahedral-symmetric surfaces
- Nuclear ‘diamonds’ do not resemble diamonds very much!

Mean Field Theory: Tetrahedral Gaps

Double group T_d^D has two 2-dimensional - and one 4-dimensional irreducible representations: Three distinct families of nucleon levels

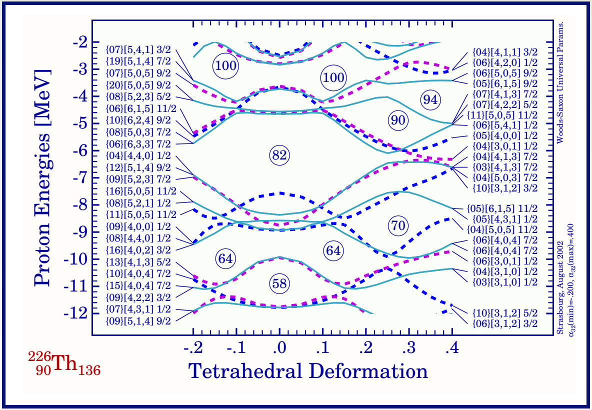

Full lines ↔ 4-dimensional irreducible representations - marked with double Nilsson labels. Observe huge gaps at $Z = 64, 70, 90 - 94, 100$.

Mean Field Theory: Tetrahedral Gaps

Double group T_d^D has two 2-dimensional - and one 4-dimensional irreducible representations: Three distinct families of nucleon levels

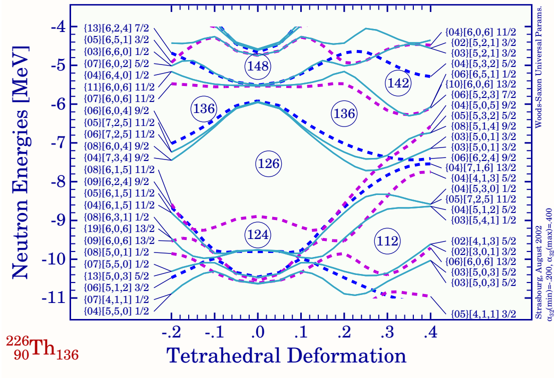

Full lines ↔ 4-dimensional irreducible representations - marked with double Nilsson labels. Observe huge gaps at N = 112, 136, 142.

Symmetries Are the Factors Determining Stability*) of Atomic Nuclei

*) *... by imposing hindrance mechanisms*

Symmetries Are the Factors Determining Stability*) of Atomic Nuclei

Nuclear mean field theory and group representation theory which are used in this research belong to the most powerful tools of nuclear structure theory arsenal

*) *... by imposing hindrance mechanisms*

Possible Measurable Signs
of
Nuclear Tetrahedral Symmetry

Quadrupole Moments vs. Pure Octupole Shapes

- Nuclear surface Σ is defined in terms of multipole deformations:

$$\Sigma: \quad R(\vartheta,\varphi) = R_0\left[1 + \sum_\lambda \sum_\mu \alpha_{\lambda\mu} Y_{\lambda\mu}(\vartheta,\varphi)\right]$$

- Given uniform density $\rho_\Sigma(\vec{r})$ defined using the surface Σ

$$\rho_\Sigma(\vec{r}) = \begin{cases} \rho_0 : & \vec{r} \in \Sigma \\ 0 : & \vec{r} \notin \Sigma \end{cases}$$

- Express the multipole moments as usual by

$$Q_{\lambda\mu} = \int \rho_\Sigma(\vec{r})\, r^\lambda\, Y_{\lambda\mu}\, d^3\vec{r}$$

- We can calculate the quadrupole moments as functions of $\alpha_{3\mu}$

One can demonstrate that among $\lambda = 3$ (octupole) deformations only α_{32} leads to $Q_2 \equiv 0$ and thus $B(E2) = 0$!

Quadrupole Moments vs. Pure Octupole Shapes

- Nuclear surface Σ is defined in terms of multipole deformations:

$$\Sigma : \quad R(\vartheta,\varphi) = R_0 \left[1 + \sum_\lambda \sum_\mu \alpha_{\lambda\mu} Y_{\lambda\mu}(\vartheta,\varphi)\right]$$

- Given uniform density $\rho_\Sigma(\vec{r})$ defined using the surface Σ

$$\rho_\Sigma(\vec{r}) = \begin{cases} \rho_0 : & \vec{r} \in \Sigma \\ 0 : & \vec{r} \notin \Sigma \end{cases}$$

- Express the multipole moments as usual by

$$Q_{\lambda\mu} = \int \rho_\Sigma(\vec{r})\, r^\lambda Y_{\lambda\mu}\, d^3\vec{r}$$

- We can calculate the quadrupole moments as functions of $\alpha_{3\mu}$

One can demonstrate that among $\lambda = 3$ (octupole) deformations only α_{32} leads to $Q_2 \equiv 0$ and thus $B(E2) = 0$!

Quadrupole Moments vs. Pure Octupole Shapes

- Nuclear surface Σ is defined in terms of multipole deformations:

$$\Sigma : \quad R(\vartheta, \varphi) = R_0 \left[1 + \sum_\lambda \sum_\mu \alpha_{\lambda\mu} Y_{\lambda\mu}(\vartheta, \varphi)\right]$$

- Given uniform density $\rho_\Sigma(\vec{r}\,)$ defined using the surface Σ

$$\rho_\Sigma(\vec{r}\,) = \begin{cases} \rho_0 : & \vec{r} \in \Sigma \\ 0 : & \vec{r} \notin \Sigma \end{cases}$$

- Express the multipole moments as usual by

$$Q_{\lambda\mu} = \int \rho_\Sigma(\vec{r}\,)\, r^{\lambda}\, Y_{\lambda\mu}\, d^3\vec{r}$$

- We can calculate the quadrupole moments as functions of $\alpha_{3\mu}$

One can demonstrate that among $\lambda = 3$ (octupole) deformations only α_{32} leads to $Q_2 \equiv 0$ and thus $B(E2) = 0$!

Quadrupole Moments vs. Pure Octupole Shapes

- Nuclear surface Σ is defined in terms of multipole deformations:

$$\Sigma: \quad R(\vartheta, \varphi) = R_0 \left[1 + \sum_\lambda \sum_\mu \alpha_{\lambda\mu} Y_{\lambda\mu}(\vartheta, \varphi)\right]$$

- Given uniform density $\rho_\Sigma(\vec{r})$ defined using the surface Σ

$$\rho_\Sigma(\vec{r}) = \begin{cases} \rho_0 : & \vec{r} \in \Sigma \\ 0 : & \vec{r} \notin \Sigma \end{cases}$$

- Express the multipole moments as usual by

$$Q_{\lambda\mu} = \int \rho_\Sigma(\vec{r})\, r^\lambda\, Y_{\lambda\mu}\, d^3\vec{r}$$

- We can calculate the quadrupole moments as functions of $\alpha_{3\mu}$

One can demonstrate that among $\lambda = 3$ (octupole) deformations only α_{32} leads to $Q_2 \equiv 0$ and thus $B(E2) = 0$!

Quadrupole Moments vs. Pure Octupole Shapes

- Nuclear surface Σ is defined in terms of multipole deformations:

$$\Sigma : \quad R(\vartheta, \varphi) = R_0 \left[1 + \sum_\lambda \sum_\mu \alpha_{\lambda\mu} Y_{\lambda\mu}(\vartheta, \varphi)\right]$$

- Given uniform density $\rho_\Sigma(\vec{r}\,)$ defined using the surface Σ

$$\rho_\Sigma(\vec{r}\,) = \begin{cases} \rho_0 : & \vec{r} \in \Sigma \\ 0 : & \vec{r} \notin \Sigma \end{cases}$$

- Express the multipole moments as usual by

$$Q_{\lambda\mu} = \int \rho_\Sigma(\vec{r}\,)\, r^{\lambda}\, Y_{\lambda\mu}\, d^3\vec{r}$$

- We can calculate the quadrupole moments as functions of $\alpha_{3\mu}$

One can demonstrate that among $\lambda = 3$ (octupole) deformations only α_{32} leads to $Q_2 \equiv 0$ and thus $B(E2) = 0$!

Quadrupole Moments vs. Pure Octupole Shapes

Indeed, for microscopically calculated quadrupole moments (W.S.)

$$Q_{20}(\alpha_{3\mu}) = \int \Psi^*_{WS}(\tau)\hat{Q}_{20}\Psi_{WS}(\tau)d\tau$$

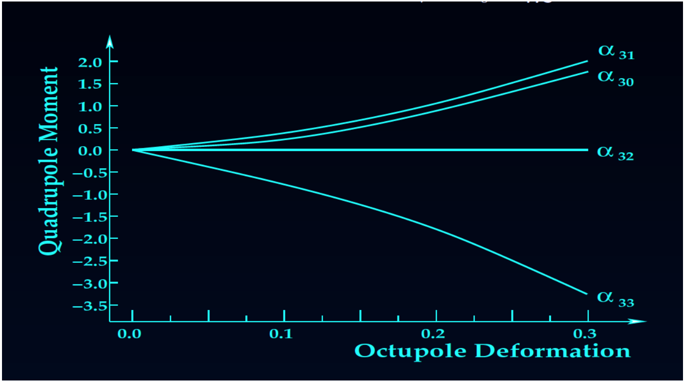

Observe that $Q_{20}(\alpha_{32})$ vanishes identically at T_d-symmetric shapes

The Notion of Isomeric Bands

Similarly one demonstrates that tetrahedral shapes induce B(E1)=0

One shows that the analogous rules apply for octahedral symmetry

Once those symmetries are present one may expect the presence of numerous isomers since B(E2) and B(E1) at the exact tetrahedral and/or octahedral symmetry limits – vanish!

As the result, one expects series of long living (isomeric) states with unprecedented parabolic energy-spin relation

Isomers at: $E_I \propto I(I+1) \leftarrow$ Isomeric Bands

The Notion of Isomeric Bands

Similarly one demonstrates that tetrahedral shapes induce B(E1)=0

One shows that the analogous rules apply for octahedral symmetry

Once those symmetries are present one may expect the presence of numerous isomers since B(E2) and B(E1) at the exact tetrahedral and/or octahedral symmetry limits – vanish!

As the result, one expects series of long living (isomeric) states with unprecedented <u>parabolic</u> energy-spin relation

Isomers at: $E_I \propto I(I+1) \leftarrow$ **Isomeric Bands**

Rotating High-Rank Symmetric Nuclei Seen Through Group-Representation Theory

[Symmetry Properties of Quantum Rotors]

Reminders: Group and Point Group Theories

• Consider a point-group symmetry characterised by group G. The SO(3)-group representation of rotor states, $D^{(I\pi)}$, with given I^π, can be decomposed in terms of irreducible representations D_i of the concerned point-group G:

$$D^{(I\pi)} = \sum_{i=1}^{M} a_i^{(I\pi)} D_i,$$

where the so-called multiplicity coefficients, $a_i^{(I\pi)}$, satisfy *)

$$a_i^{(I\pi)} = \frac{1}{N_G} \sum_{R\in G} \chi_{(I\pi)}(R)\chi_i(R) = \frac{1}{N_G} \sum_{\alpha=1}^{M} n_\alpha \chi_{(I\pi)}(g_\alpha)\chi_i(g_\alpha)$$

→ $\chi_{(I\pi)}$ - characters of the reducible representation $D^{(I\pi)}$ of the SO(3)-group;
→ χ_i - characters of the irreducible representation D_i of a point group;
→ N_G - order of the group G;
→ g - group element;
→ n_α - the number of elements in the class α, whose representative element is g_α.

——

*) M. Hamermesh, *Group Theory and Its Application to Physical Problems*, Addison-Wesley Publishing Company, Inc., 1962

*) Tagami, Shimizu, Dudek, Phys. Rev. C**87**, 054306 (2013), DOI: `https://doi.org/10.1103/PhysRevC.87.054306`

Example: Tetrahedral T_d-Group

- Tetrahedral group has 5 irreducible representations, and 5 classes
- The representative elements $\{g\}$ are: $E, C_2\,(= S_4^2), C_3, \sigma_d, S_4$
- The characters of irreducible representations of T_d are listed below

T_d	E	$C_3(8)$	$C_2(3)$	$\sigma_d(2)$	$S_4(6)$
A_1	1	1	1	1	1
A_2	1	1	1	−1	−1
E	2	−1	2	0	0
F_1	3	0	−1	−1	1
F_2	3	0	−1	1	−1

- The characters $\chi_{(I\pi)}(g_\alpha)$ for the SO(3) representations are as follows:

$$\chi_{(I\pi)}(E) = 2I+1, \quad \chi_{(I\pi)}(C_n) = \sum_{K=-I}^{I} e^{\frac{2\pi K}{n} i}, \quad \Rightarrow$$

$$\chi_{(I\pi)}(\sigma_d) = \pi \times \chi_{(I\pi)}(C_2), \; \chi_{(I\pi)}(S_4) = \pi \times \chi_{(I\pi)}(C_4)$$

- Multiplicity coefficients can be calculated in an elementary fashion

$$a_i^{(I\pi)} = \frac{1}{N_G} \sum_{g \in G} \chi_{(I\pi)}(g)\chi_i(g) = \frac{1}{N_G} \sum_{\alpha=1}^{M} n_\alpha \chi_{(I\pi)}(g_\alpha)\chi_i(g_\alpha);$$

Resulting Prediction of the Structure of T_d-Bands

- The number of states $a_i^{(I\pi)}$ within five irreducible representations. If $a_i^{(I\pi)} = 0 \;\rightarrow$ states not allowed; $a_i^{(I\pi)} = 2 \;\rightarrow$ doubly degenerate, etc.

I^+	0^+	1^+	2^+	3^+	4^+	5^+	6^+	7^+	8^+	9^+	10^+
A_1	1	0	0	0	1	0	1	0	1	1	1
A_2	0	0	0	1	0	0	1	1	0	1	1
E	0	0	1	0	1	1	1	1	2	1	2
$F_1(T_1)$	0	1	0	1	1	2	1	2	2	3	2
$F_2(T_2)$	0	0	1	1	1	1	2	2	2	2	3
I^-	0^-	1^-	2^-	3^-	4^-	5^-	6^-	7^-	8^-	9^-	10^-
A_1	0	0	0	1	0	0	1	1	0	1	1
A_2	1	0	0	0	1	0	1	0	1	1	1
E	0	0	1	0	1	1	1	1	2	1	2
F_1	0	0	1	1	1	1	2	2	2	2	3
F_2	0	1	0	1	1	2	1	2	2	3	2

- In this way we find the spin-parity sequence for A_1-representation

$$A_1 : \quad 0^+, 3^-, 4^+, 6^+, 6^-, 7^-, 8^+, 9^+, 9^-, 10^+, 10^-, 11^-, 2\times 12^+, 12^-, \cdots$$

- **This is the group-theory prediction of the spin-parity structure of the tetrahedral g.s.b.**

Tetrahedral Bands Are Not Like the Others!

As we have shown using the methods of the point-group representation theory that, for instance, rotational bands based on 0^+ "T_d ground-state" have the structure:

$$A_1: \quad 0^+, 3^-, 4^+, 6^+, 6^-, 7^-, 8^+, 9^+, 9^-, 10^+, 10^-, 11^-, 2\times 12^+, 12^-, \cdots$$

and NOT

$$\boldsymbol{I^\pi: \quad 0^+, 2^+, 4^+, 6^+, 8^+, 10^+, 12^+, \cdots}$$

Tetrahedral Bands Are Not Like the Others!

As we have shown using the methods of the point-group representation theory that, for instance, rotational bands based on 0^+ "T_d ground-state" have the structure:

$$A_1: \quad 0^+, 3^-, 4^+, 6^+, 6^-, 7^-, 8^+, 9^+, 9^-, 10^+, 10^-, 11^-, 2\times 12^+, 12^-, \cdots$$

and NOT

$$\boldsymbol{I^\pi: \quad 0^+, 2^+, 4^+, 6^+, 8^+, 10^+, 12^+, \cdots}$$

Similarly there are **no analogies** of the "octupole bands"

$$\boldsymbol{I^\pi: \quad 3^-, 5^-, 7^-, 9^-, 11^-, 13^-, 15^-, \cdots}$$

Quantum Rotors: Tetrahedral vs. Octahedral

- The tetrahedral $\mathrm{T_d}$ symmetry group has 5 irreducible representations
- The ground-state $I^\pi = 0^+$ belongs to A_1 representation given by:

$$\mathrm{A}_1: \quad \underbrace{0^+, 3^-, 4^+, \underbrace{(6^+, 6^-)}_{\text{doublet}}, 7^-, 8^+, \underbrace{(9^+, 9^-)}_{\text{doublet}}, \underbrace{(10^+, 10^-)}_{\text{doublet}}, 11^-, \underbrace{2\times 12^+, 12^-}_{\text{triplet}}, \cdots}_{\textbf{Forming a common parabola}}$$

- There are no states with spins $I = 1, 2$ and 5. We have parity doublets: $I = 6, 9, 10 \ldots$, at energies: $E_{6^-} \approx E_{6^+}$, $E_{9^-} \approx E_{9^+}$, etc.

Quantum Rotors: Tetrahedral vs. Octahedral

- The tetrahedral $\mathrm{T_d}$ symmetry group has 5 irreducible representations
- The ground-state $I^\pi = 0^+$ belongs to A_1 representation given by:

$$\underbrace{\mathrm{A}_1: \quad 0^+, 3^-, 4^+, \underbrace{(6^+, 6^-)}_{\text{doublet}}, 7^-, 8^+, \underbrace{(9^+, 9^-)}_{\text{doublet}}, \underbrace{(10^+, 10^-)}_{\text{doublet}}, 11^-, \underbrace{2 \times 12^+, 12^-}_{\text{triplet}}, \cdots}_{\textbf{Forming a common parabola}}$$

- There are no states with spins $I = 1, 2$ and 5. We have parity doublets: $I = 6, 9, 10 \ldots$, at energies: $E_{6^-} \approx E_{6^+}$, $E_{9^-} \approx E_{9^+}$, etc.

- One shows the analogue structures for the octahedral $\mathrm{O_h}$ symmetry

$$\underbrace{A_{1g}: \; 0^+, 4^+, 6^+, 8^+, 9^+, 10^+, \; \ldots, \quad I^\pi = I^+}_{\textbf{Forming a common parabola}}$$

$$\underbrace{A_{2u}: \; 3^-, 6^-, 7^-, 9^-, 10^-, 11^-, \ldots, \; I^\pi = I^-}_{\textbf{Forming another (common) parabola}}$$

Experimental Data Selection for T_d

About criteria for the experimental data search

- Central condition followed: Nuclear states with exact high-rank symmetries produce neither dipole-, nor quadrupole moments

- Such states neither emit any collective/strong E1/E2 transitions nor can be fed by such transitions → focus on the nuclear processes

- Therefore we decided to focus first of all on the nuclei which can be populated with a big number of nuclear reactions since we may expect that - in such nuclei - the states sought exist in the literature

- We had verified that the nucleus ^{152}Sm can be produced by about 25 nuclear reactions, whereas surrounding nuclei can be produced typically with about a dozen but usually much fewer reactions only

- Energy-wise – tetrahedral bands form regular sequences

$$E_I \propto AI^2 + BI + C$$

Experimental Data Selection for T_d

About criteria for the experimental data search

- Central condition followed: Nuclear states with exact high-rank symmetries produce neither dipole-, nor quadrupole moments

- Such states neither emit any collective/strong E1/E2 transitions nor can be fed by such transitions → focus on the nuclear processes

- Therefore we decided to focus first of all on the nuclei which can be populated with a big number of nuclear reactions since we may expect that - in such nuclei - the states sought exist in the literature

- We had verified that the nucleus ^{152}Sm can be produced by about 25 nuclear reactions, whereas surrounding nuclei can be produced typically with about a dozen but usually much fewer reactions only

- Energy-wise – tetrahedral bands form regular sequences

$$E_I \propto AI^2 + BI + C$$

Experimental Data Selection for T_d

About criteria for the experimental data search

• Central condition followed: Nuclear states with exact high-rank symmetries produce neither dipole-, nor quadrupole moments

• Such states neither emit any collective/strong E1/E2 transitions nor can be fed by such transitions → focus on the nuclear processes

• Therefore we decided to focus first of all on the nuclei which can be populated with a big number of nuclear reactions since we may expect that - in such nuclei - the states sought exist in the literature

• We had verified that the nucleus ^{152}Sm can be produced by about 25 nuclear reactions, whereas surrounding nuclei can be produced typically with about a dozen but usually much fewer reactions only

• Energy-wise – tetrahedral bands form regular sequences

$$E_I \propto AI^2 + BI + C$$

Experimental Data Selection for T_d

About criteria for the experimental data search

- Central condition followed: Nuclear states with exact high-rank symmetries produce neither dipole-, nor quadrupole moments

- Such states neither emit any collective/strong E1/E2 transitions nor can be fed by such transitions → focus on the nuclear processes

- Therefore we decided to focus first of all on the nuclei which can be populated with a big number of nuclear reactions since we may expect that - in such nuclei - the states sought exist in the literature

- We had verified that the nucleus ^{152}Sm can be produced by about 25 nuclear reactions, whereas surrounding nuclei can be produced typically with about a dozen but usually much fewer reactions only

- Energy-wise – tetrahedral bands form regular sequences

$$E_I \propto AI^2 + BI + C$$

Experimental Data Selection for T_d

About criteria for the experimental data search

- Central condition followed: Nuclear states with exact high-rank symmetries produce neither dipole-, nor quadrupole moments

- Such states neither emit any collective/strong E1/E2 transitions nor can be fed by such transitions → focus on the nuclear processes

- Therefore we decided to focus first of all on the nuclei which can be populated with a big number of nuclear reactions since we may expect that - in such nuclei - the states sought exist in the literature

- We had verified that the nucleus ^{152}Sm can be produced by about 25 nuclear reactions, whereas surrounding nuclei can be produced typically with about a dozen but usually much fewer reactions only

- Energy-wise – tetrahedral bands form regular sequences

$$E_I \propto AI^2 + BI + C$$

Announcement of the Discovery – Part I

PHYSICAL REVIEW C VOLUME 97, 021302(R) FEBRUARY 2018

Spectroscopic criteria for identification of nuclear tetrahedral and octahedral symmetries: Illustration on a rare earth nucleus

J. Dudek, D. Curien, I. Dedes, K. Mazurek, S. Tagami, Y. R. Shimizu and T. Bhattacharjee

(Received 8 June 2017)

We formulate criteria for identification of the nuclear tetrahedral and octahedral symmetries and illustrate for the first time their possible realization in a rare earth nucleus ^{152}Sm. We use realistic nuclear mean-field theory calculations with the phenomenological macroscopic-microscopic method, the Gogny-Hartree-Fock-Bogoliubov approach, and general point-group theory considerations to guide the experimental identification method as illustrated on published experimental data. Following group theory the examined symmetries imply the existence of exotic rotational bands on whose properties the spectroscopic identification criteria are based. These bands may contain simultaneously states of even and odd spins, of both parities and parity doublets at well-defined spins. In the exact-symmetry limit those bands involve no E2 transitions. We show that coexistence of tetrahedral and octahedral deformations is essential when calculating the corresponding energy minima and surrounding barriers, and that it has a characteristic impact on the rotational bands. The symmetries in question imply the existence of long-lived shape isomers and, possibly, new waiting point nuclei-impacting the nucleosynthesis processes in astrophysics – and an existence of 16-fold degenerate particle-hole excitations.

Perfect Parabolas Represent Experimental Results

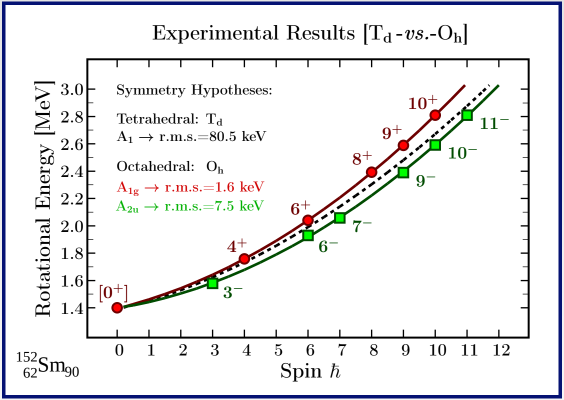

- Sequences represent **coexistence between tetrahedral and octahedral symmetries**.

Curves represent the parabolic fit and are *not* meant to guide the eye.
This is the first evidence of T_d (dashed) and O_h based on the experimental data

Perfect Parabolas Represent Experimental Results

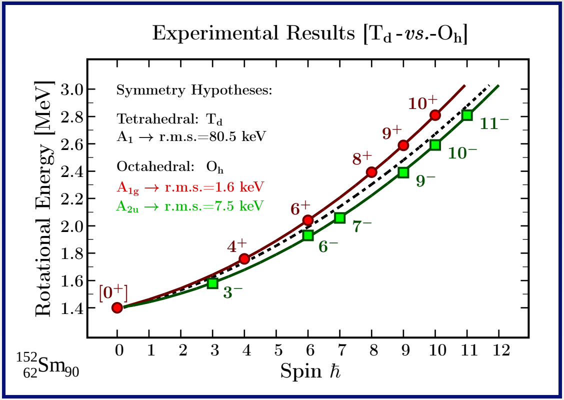

FROM: **Spectroscopic criteria for identification of nuclear tetrahedral and octahedral symmetries: Illustration on a rare earth nucleus**

J. Dudek et al., PHYSICAL REVIEW C 97, 021302(R) (2018)

[DOI: https://doi.org/10.1103/PhysRevC.97.021302]

Part 3

About Exotic Shape-Instabilities in Actinides

PHYSICAL REVIEW C VOLUME 49, NUMBER 3 MARCH 1994

Deformed atomic nuclei with degeneracies of the nucleonic levels higher than 2

Xunjun Li and Jerzy Dudek

Centre de Recherches Nucléaires, Institut National de Physique Nucléaire et de Physique des Particules du Centre National de la Recherche Scientifique, Université Louis Pasteur,
Boite Postale 20, F-67037 Strasbourg Cedex2, France

(Received 19 October 1993)

As it is well known, the single-nucleonic levels in a nucleus manifest either the Kramers degeneracy $d = 2$ or, if a nucleus is spherical, a trivial "magnetic" degeneracy $d = 2j + 1$. It will be shown using the results of the realistic total nuclear energy calculations that a possibility of fourfold degenerate nucleonic levels exists in a number of $N \sim 136$ isotones due to their high intrinsic symmetry. Those exotic states are predicted to be isomeric; they lie only a few hundreds of keV above the ground state. Other possible nuclear regions where the same mechanism may take place are indicated.

30 Years Back: Original vs. Newest Forms

- Left: Single particle levels from Phys. Rev. C49 R1250 (1994);
  Right: Modern version of parameters, so-called "universal-compact"

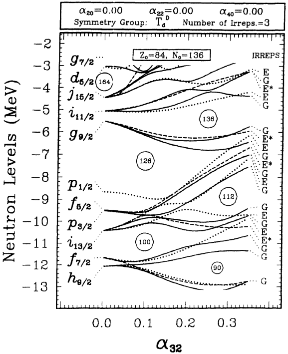

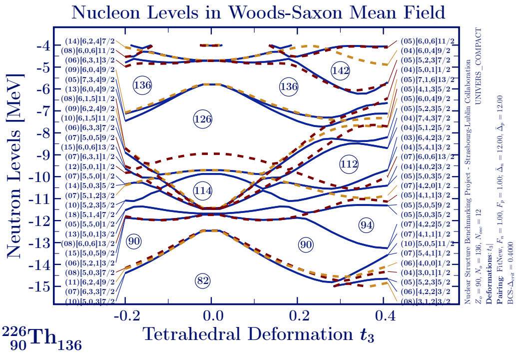

- Observe correspondence between the tetrahedral magic-number predictions: $N_t^{\nu} = 90, 94, 112, 136, 142 \rightarrow$ historical vs. modern

30 Years Back: Original vs. Newest Forms

- Left: Single particle levels from Phys. Rev. C49 R1250 (1994);
  Right: Modern version of parameters, so-called "universal-compact"

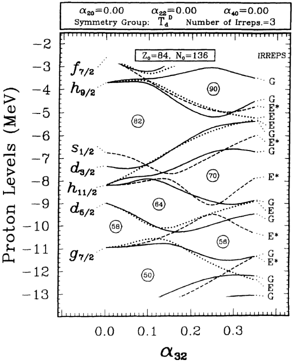

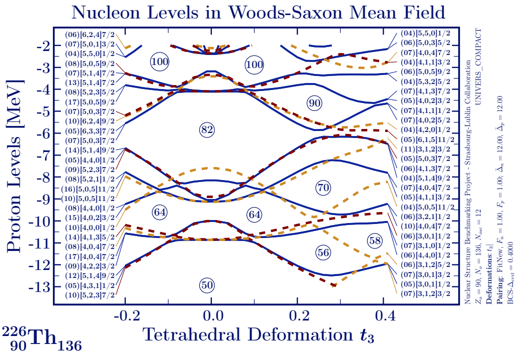

- Observe correspondence between the tetrahedral magic-number predictions: $N_t^{\pi} = 56, 58, 70, 90 \rightarrow$ historical vs. modern

30 Years Back: Original vs. Newest Forms

• The first traces of the octahedral symmetry – although the authors did not address it at that time: “unwanted effect of hexadecapole deformation”

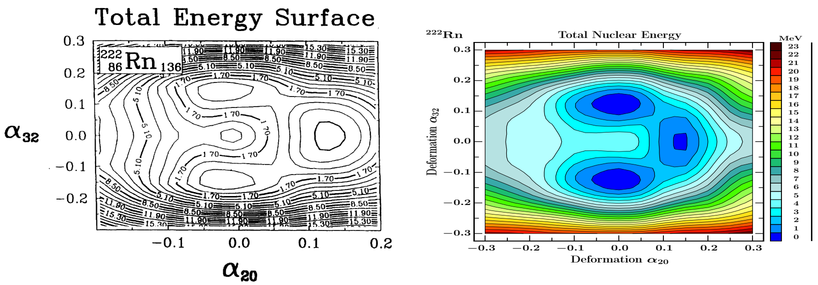

• **What is presented here as unwanted effect of hexadecapole deformation is in fact the “very much wanted” effect of the octahedral symmetry:**

$$\alpha_{40} \to o_1 \equiv \{\alpha_{40};\ \alpha_{4,\pm4} = \sqrt{5/14}\cdot\alpha_{40}\},$$

and in fact its effect lowers the energy considerably

Path to Exotic Symmetries: Begin with Spherical ^{208}Pb

- Consider ^{208}Pb nucleus, doubly magic, among the most stable, spherical, ...
- The first excited state is an $I^{\pi} = 3^{-}$, traditionally associated with the pear-shape $Y_{\lambda=3,\mu=0}$-oscillations
- Other negative parity octupole modes are generated by multipolarities $Y_{\lambda=3,\mu\neq 0}$

Multipolarity $\alpha_{\lambda=3,\mu}$	Point Group
α_{30}	$C_{\infty v}$
α_{31}	C_{2v}
α_{32}	T_d
α_{33}	D_{3h}

- One can demonstrate that these are the corresponding Point Groups

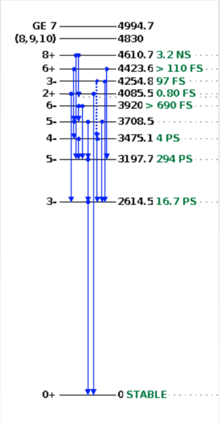

^{208}Pb Level Scheme from NNDC; 3^{-} state traditionally associated with the octupole (pear-shape) oscillations

What structural mechanisms are expected to bring the $I^\pi = 3^-$ vibrations to the lowest position in the spectrum?

More generally, what are the shell mechanisms responsible of lowering the negative parity collective states?

We Begin With the Octupole Shell-Structures

- We will overview the $\lambda = 3$ deformation shell effects in the Pb region

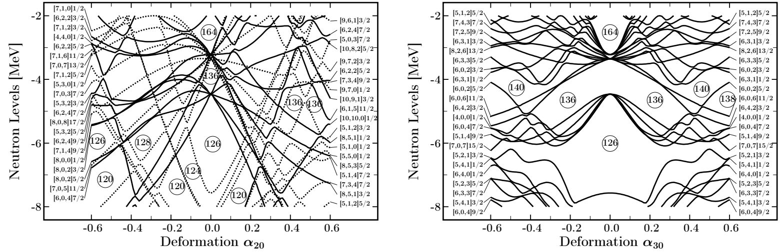

- For Pb-nuclei, thus at fixed $Z = 82$, the variation in octupole effects originates from the evolution of the neutron shell structure – right plot

- Octupole shell gap opening at $N = 136$: repulsive interaction between the $2g_{9/2}$ ($N_{\text{shell}} = 6$) and the intruder $1j_{15/2}$ ($N_{\text{shell}} = 7$)

Shell Structures at $N = 136 \rightarrow \alpha_{30}, \alpha_{31}, \alpha_{32}, \alpha_{33}$

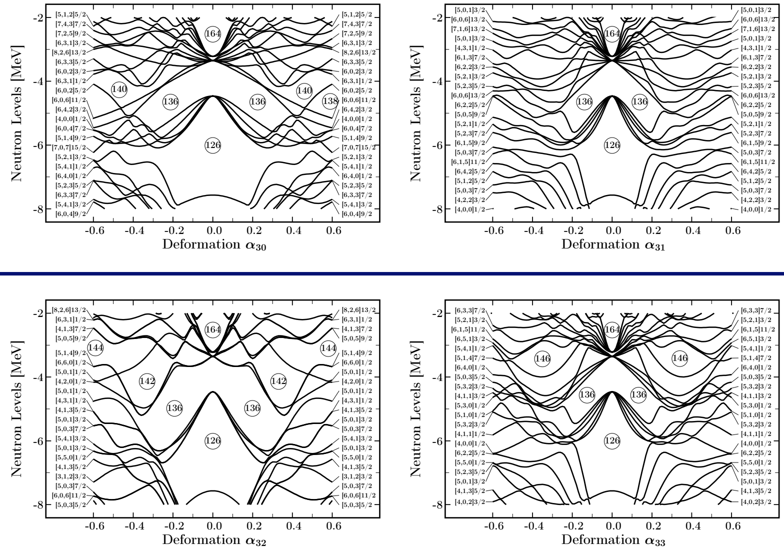

We conclude that $N = 136$ plays the role of a special octupole magic-number and this – for all the 4 octupole multipolarities

*) I. Hamamoto, B. Mottelson, H. Xie, and X. Z. Zhang,
Z. Phys. D - Atoms, Molecules and Clusters 21, 163-175 (1991)

We conclude that $N = 136$ plays the role of a special octupole magic-number and this – for all the 4 octupole multipolarities

Consequences in terms of the nuclear structure*)

---

*) I. Hamamoto, B. Mottelson, H. Xie, and X. Z. Zhang,
Z. Phys. D - Atoms, Molecules and Clusters 21, 163-175 (1991)

Evolution of Pear-Shape Instabilities: ^{208}Pb

- Projection on the $(\alpha_{20}, \alpha_{30})$-plane minimised over $(\alpha_{22}, \alpha_{40})$ for ^{208}Pb

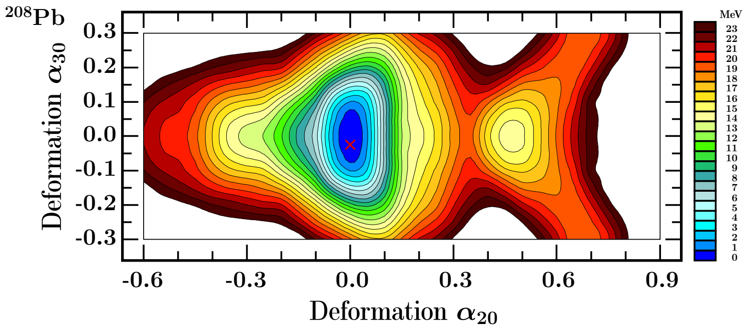

Evolution of Pear-Shape Instabilities: ^{210}Pb

- Projection on the $(\alpha_{20}, \alpha_{30})$-plane minimised over $(\alpha_{22}, \alpha_{40})$ for ^{210}Pb

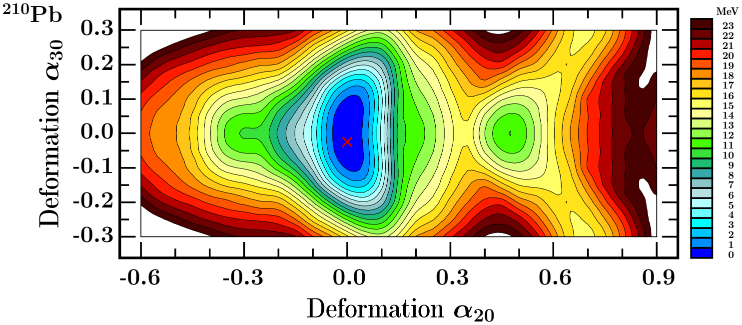

Evolution of Pear-Shape Instabilities: ^{212}Pb

- Projection on the $(\alpha_{20}, \alpha_{30})$-plane minimised over $(\alpha_{22}, \alpha_{40})$ for ^{212}Pb

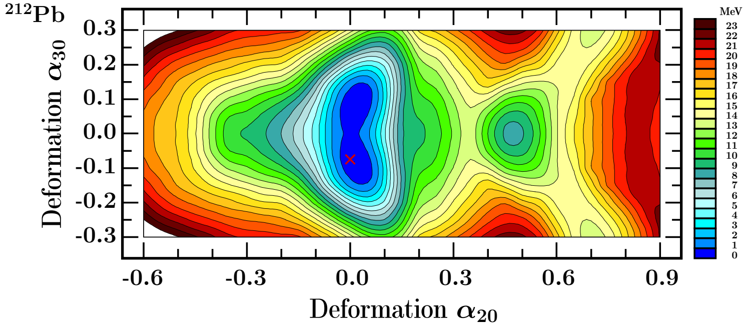

Evolution of Pear-Shape Instabilities: ^{214}Pb

- Projection on the $(\alpha_{20}, \alpha_{30})$-plane minimised over $(\alpha_{22}, \alpha_{40})$ for ^{214}Pb

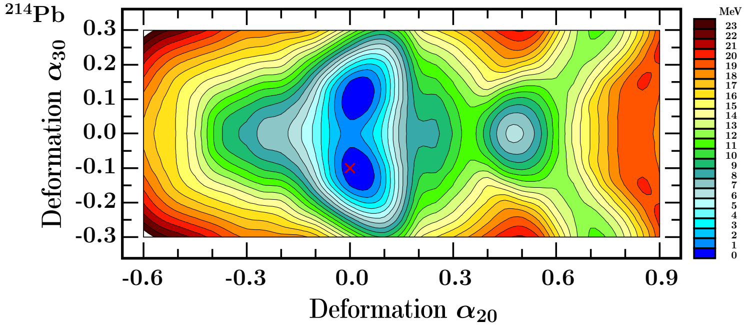

Evolution of Pear-Shape Instabilities: ^{216}Pb

- Projection on the $(\alpha_{20}, \alpha_{30})$-plane minimised over $(\alpha_{22}, \alpha_{40})$ for ^{216}Pb

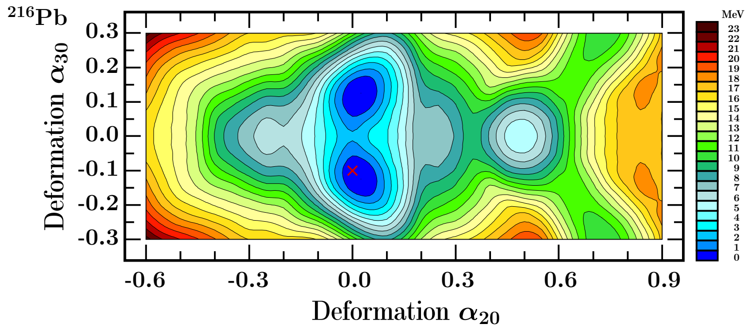

Evolution of Pear-Shape Instabilities: ^{218}Pb

- Projection on the $(\alpha_{20}, \alpha_{30})$-plane minimised over $(\alpha_{22}, \alpha_{40})$ for ^{218}Pb

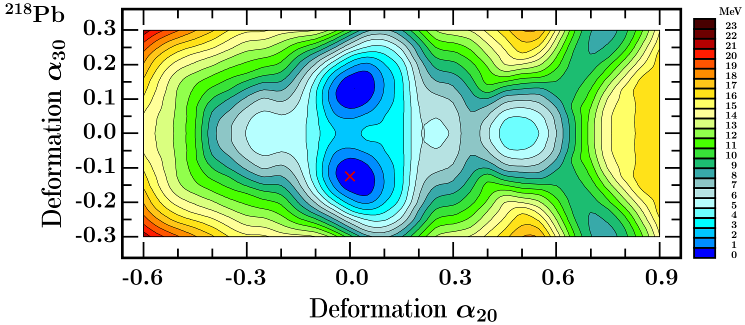

Comparison: $\lambda = 3$ Susceptibility in ^{218}Pb Region

- Projection on the $(\alpha_{20}, \alpha_{3\mu})$-plane minimised over $(\alpha_{22}, \alpha_{40})$ for ^{218}Pb

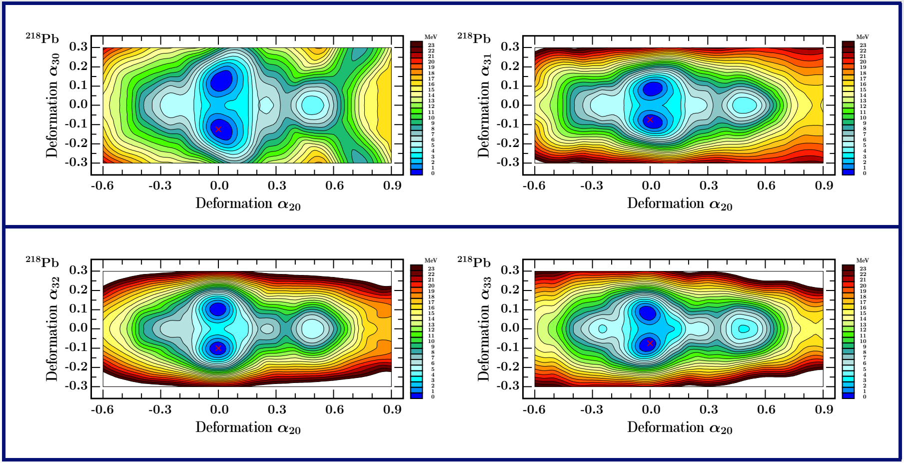

Observations about Heavy Pb Isotopes

• Appearance of strongly pronounced octupole minima for increasing neutron number → the highest barriers separating double minima arriving at $N = 136$

Observations about Heavy Pb Isotopes

• Appearance of strongly pronounced octupole minima for increasing neutron number → the highest barriers separating double minima arriving at $N = 136$

• Comparison of the 2D-projections onto $(\alpha_{20}, \alpha_{3\mu})$-planes shows that four octupole deformations produce well-pronounced double minima at $\alpha_{20} = 0.0$ and $\alpha_{3\mu} \neq 0.0$ → The loss of sphericity at $\boldsymbol{\lambda \neq 2}$ multipolarity ↔ **exoticity**

Observations about Heavy Pb Isotopes

• Appearance of strongly pronounced octupole minima for increasing neutron number → the highest barriers separating double minima arriving at $N = 136$

• Comparison of the 2D-projections onto $(\alpha_{20}, \alpha_{3\mu})$-planes shows that four octupole deformations produce well-pronounced double minima at $\alpha_{20} = 0.0$ and $\alpha_{3\mu} \neq 0.0$ → The loss of sphericity at **$\lambda \neq 2$** multipolarity ↔ **exoticity**

• The strongest octupole effect for ^{218}Pb ($N = 136$) corresponds to

α_{32} ↔ Tetrahedral Symmetry T_d

Observations about Heavy Pb Isotopes

• Appearance of strongly pronounced octupole minima for increasing neutron number → the highest barriers separating double minima arriving at $N = 136$

• Comparison of the 2D-projections onto $(\alpha_{20}, \alpha_{3\mu})$-planes shows that four octupole deformations produce well-pronounced double minima at $\alpha_{20} = 0.0$ and $\alpha_{3\mu} \neq 0.0$ → The loss of sphericity at **$\lambda \neq 2$** multipolarity ↔ **exoticity**

• The strongest octupole effect for ^{218}Pb ($N = 136$) corresponds to

$$\alpha_{32} \leftrightarrow \textbf{Tetrahedral Symmetry } \mathbf{T_d}$$

• Since these heavy Pb-isotopes represent exotic nuclei, they do not have a lot of experimental data known

Observations about Heavy Pb Isotopes

• Appearance of strongly pronounced octupole minima for increasing neutron number → the highest barriers separating double minima arriving at $N = 136$

• Comparison of the 2D-projections onto $(\alpha_{20}, \alpha_{3\mu})$-planes shows that four octupole deformations produce well-pronounced double minima at $\alpha_{20} = 0.0$ and $\alpha_{3\mu} \neq 0.0$ → The loss of sphericity at $\boldsymbol{\lambda \neq 2}$ multipolarity ↔ **exoticity**

• The strongest octupole effect for ^{218}Pb ($N = 136$) corresponds to

$$\boldsymbol{\alpha_{32} \leftrightarrow \textbf{Tetrahedral Symmetry } T_d}$$

• Since these heavy Pb-isotopes represent exotic nuclei, they do not have a lot of experimental data known

⇒ We check the $Z > 82$ nuclei since they are easier to access experimentally

Exotic Symmetries for $Z > 82$ Nuclei: ^{222}Rn

- Projection on the $(\alpha_{20}, \alpha_{3\mu})$-plane minimised over $(\alpha_{22}, \alpha_{40})$

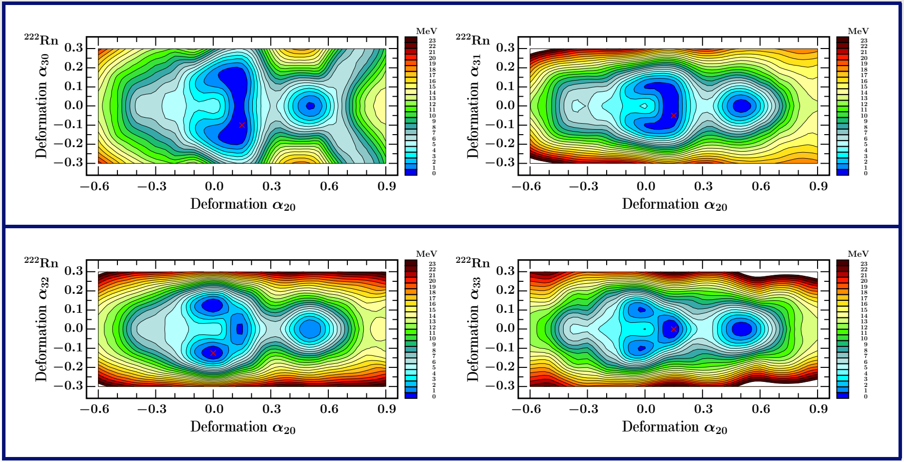

Observations

• Appearance of strongly pronounced octupole minima in nuclei with $Z > 82$, especially those close to $N = 136$

• In contrast to the Pb case, some of the octupole instabilities appear for $\alpha_{20} \neq 0.0$

• This favours the experimental identification of slightly broken tetrahedral symmetry since with $B(E2) \neq 0$ one can hope for profiting from the Germanium multi-detector systems and identify, even if weak, quadrupole transitions

Observations

• Appearance of strongly pronounced octupole minima in nuclei with $Z > 82$, especially those close to $N = 136$

• In contrast to the Pb case, some of the octupole instabilities appear for $\alpha_{20} \neq 0.0$

• This favours the experimental identification of slightly broken tetrahedral symmetry since with $B(E2) \neq 0$ one can hope for profiting from the Germanium multi-detector systems and identify, even if weak, quadrupole transitions

$\Rightarrow$ What are the induced exotic molecular symmetries? $\Leftarrow$

We use Point Group and Group-Representation Theories

Synthetic View of Octupole Instabilities

- The octupole-shape deformations include $\alpha_{\lambda=3,\mu=0,1,2,3}$ thus leading to 4 independent degrees of freedom (Note: minima obtained at $\alpha_{20} = 0$)

$$\{\alpha_{30} \neq 0,\ \alpha_{31} \neq 0,\ \alpha_{32} \neq 0,\ \alpha_{33} \neq 0\}$$

- One can demonstrate that they generate **Point-Group Symmetries:**

$$\mathbf{C_{\infty v}},\quad \mathbf{C_{2v}},\quad \mathbf{T_d},\quad \mathbf{D_{3h}},\quad \textbf{respectively}$$

- It turns out that octupole static or dynamic state equilibria may lead to specific rotational band structures $\Rightarrow$ what are these structures?

Molecular (Point-Group) Symmetries - $C_{2v} \Leftrightarrow \alpha_{31}$

- **Symmetry induced by both ($\alpha_{31} \neq 0$) and ($\alpha_{20} \neq 0, \alpha_{31} \neq 0$)**

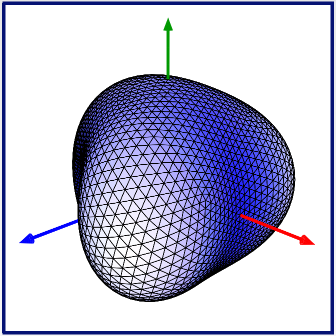

$\alpha_{31} = 0.25$

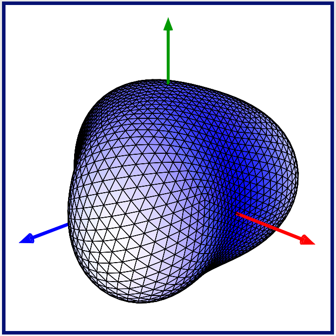

$\alpha_{20} = 0.15, \alpha_{31} = 0.25$

Nuclear C_{2v} Point Group Symmetry

Molecular (Point-Group) Symmetries - T_d & D_{2d} ⇔ α_{32}

- Symmetry induced by ($\alpha_{32} \neq 0$) and ($\alpha_{20} \neq 0, \alpha_{32} \neq 0$)

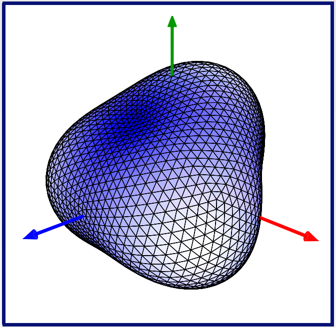

Tetrahedral T_d: $\alpha_{32} = 0.25$

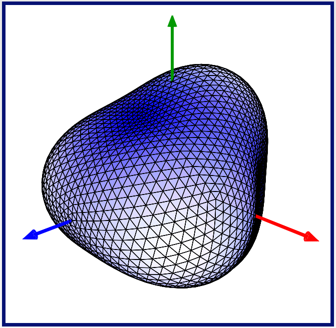

D_{2d}: $\alpha_{20} = 0.15, \alpha_{32} = 0.25$

Nuclear T_d and D_{2d} Point Group Symmetries

Molecular (Point-Group) Symmetries - $D_{3h} \Leftrightarrow \alpha_{33}$

- **Symmetry induced by both ($\alpha_{33} \neq 0$) and ($\alpha_{20} \neq 0, \alpha_{33} \neq 0$)**

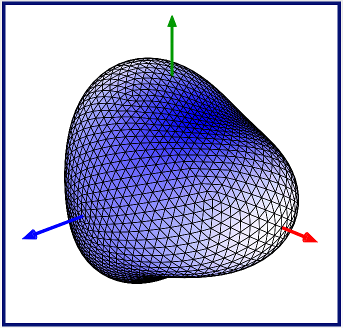

$\alpha_{33} = 0.25$

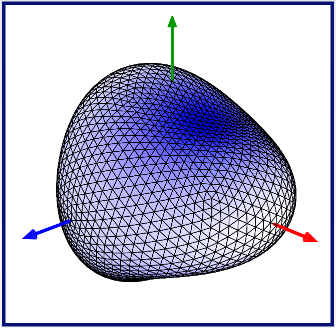

$\alpha_{20} = 0.15, \alpha_{33} = 0.25$

Nuclear D_{3h} Point Group Symmetry

How to proceed once we know the point group representing a certain symmetry of interest?

How to proceed once we know the point group representing a certain symmetry of interest?

Suggestion: Examine rotational properties of concerned nuclei with the help of the group representation theory

Reminders: E-vs-I Parabolic Dependence

- Hartree-Fock-Bogolyubov spin-parity projected: Microscopic theory result

MICROSCOPIC STUDY OF TETRAHEDRALLY SYMMETRIC . . . PHYSICAL REVIEW C **87**, 054306 (2013)

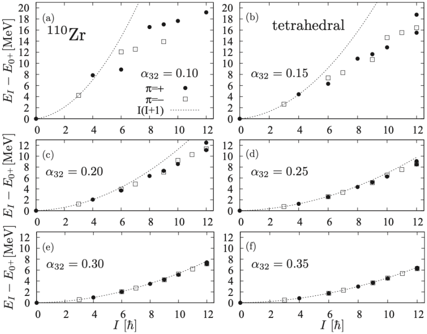

FIG. 8. Calculated spectra of tetrahedral states in ^{110}Zr with $\alpha_{32} = 0.10, 0.15, 0.20, 0.25, 0.30$, and 0.35, respectively, for (a), (b), (c), (d), (e), and (f). The figure is similar to that in Ref. [31] but only the lowest band is selected and the results for larger deformation are included. Note that almost exact degeneracies for $I = (6^+, 6^-), (9^+, 9^-), (10^+, 10^-), (2 \times 12^+, 12^-)$ states are obtained for $\alpha_{32} \geqslant 0.30$.

- $I^{\pi}_{\mathrm{T_d}} = 0^+, 3^-, 4^+, 6^{\pm}, 7^-, 8^+, 9^{\pm}, 10^{\pm}, 11^-, \ldots$ form a common parabola

Rotational Band Properties of Exotic Symmetries: T_d

The first tetrahedral symmetry evidence based on the experimental data

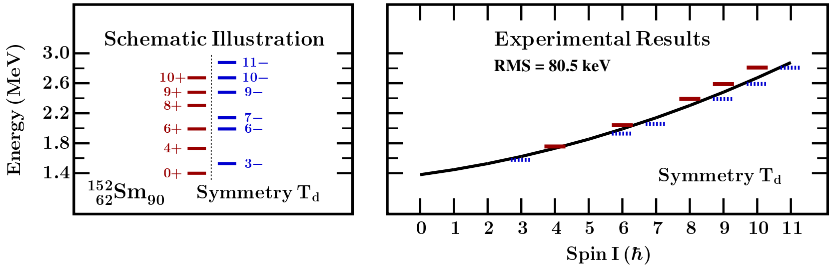

Tetrahedral Band : $I^{\pi}_{T_d} = 0^+, 3^-, 4^+, 6^{\pm}, 7^-, 8^+, 9^{\pm}, 10^{\pm}, 11^-, \ldots$

→ **Published in: J. Dudek et al., PHYSICAL REVIEW C 97, 021302(R) (2018)**
[DOI: https://doi.org/10.1103/PhysRevC.97.021302]

- **The R.M.S. of the ground-state band is 15.18 keV**

Resulting Prediction of the Structure of C_{2v}-Bands

- Multiplicity factors for the 4 irreducible representations of C_{2v}-group

I^+	0^+	1^+	2^+	3^+	4^+	5^+	6^+	7^+	8^+	9^+	10^+
A_1	1	0	2	1	3	2	4	3	5	4	6
A_2	0	1	1	2	2	3	3	4	4	5	5
B_1	0	1	1	2	2	3	3	4	4	5	5
B_2	0	1	1	2	2	3	3	4	4	5	5
I^-	0^-	1^-	2^-	3^-	4^-	5^-	6^-	7^-	8^-	9^-	10^-
A_1	0	1	1	2	2	3	3	4	4	5	5
A_2	1	0	2	1	3	2	4	3	5	4	6
B_1	0	1	1	2	2	3	3	4	4	5	5
B_2	0	1	1	2	2	3	3	4	4	5	5

- In this way we find the spin-parity sequence for A_1-representation

$$\mathrm{A}_1:\ 0^+,\ 1^-, 2\times 2^+, 2^-, 3^+, 2\times 3^-, 3\times 4^+, 2\times 4^-, 2\times 5^+, 3\times 5^-, 4\times 6^+, 4\times 6^-, \cdots$$

- Group-theory prediction of the spin-parity structure of the C_{2v} g.s.b.

G.S.B. Predictions Overview: C_{2v}, D_{2d} and D_{3h}

- Group-theory prediction of the spin-parity structure of the **C_{2v}** g.s.b. spin-parity sequence for A_1-representation

$$\mathbf{C_{2v} \to A_1 : 0^+, 1^-, 2\times 2^+, 2^-, 3^+, 2\times 3^-, 3\times 4^+, 2\times 4^-, 2\times 5^+, 3\times 5^-, 4\times 6^+, 4\times 6^-, \cdots}$$

- Group-theory prediction of the spin-parity structure of the **D_{2d}** g.s.b. spin-parity sequence for A_1-representation

$$\mathbf{D_{2d} \to A_1 : 0^+, 2^\pm, 3^-, 2\times 4^+, 4^-, 5^\pm, 2\times 6^+, 2\times 6^-, 7^+, 2\times 7^-, \cdots}$$

- Group-theory prediction of the spin-parity structure of the **D_{3h}** g.s.b. spin-parity sequence for A_1-representation

$$\mathbf{D_{3h} \to A_1 : 0^+, 2^+, 3^-, 4^\pm, 5^-, 2\times 6^+, 6^-, 7^\pm, 2\times 8^+, 8^-, \cdots}$$

G.S.B. Predictions Overview: C_{2v}, D_{2d} and D_{3h}

- Group-theory prediction of the spin-parity structure of the **C_{2v}** g.s.b. spin-parity sequence for A_1-representation

$$C_{2v} \to A_1 : 0^+, 1^-, 2\times 2^+, 2^-, 3^+, 2\times 3^-, 3\times 4^+, 2\times 4^-, 2\times 5^+, 3\times 5^-, 4\times 6^+, 4\times 6^-, \cdots$$

- Group-theory prediction of the spin-parity structure of the **D_{2d}** g.s.b. spin-parity sequence for A_1-representation

$$D_{2d} \to A_1 : 0^+, 2^\pm, 3^-, 2\times 4^+, 4^-, 5^\pm, 2\times 6^+, 2\times 6^-, 7^+, 2\times 7^-, \cdots$$

- Group-theory prediction of the spin-parity structure of the **D_{3h}** g.s.b. spin-parity sequence for A_1-representation

$$D_{3h} \to A_1 : 0^+, 2^+, 3^-, 4^\pm, 5^-, 2\times 6^+, 6^-, 7^\pm, 2\times 8^+, 8^-, \cdots$$

- **No $\Delta I = 2$ sequences !!**

Rotational Band Properties of Exotic Symmetries

- Each point group symmetry implies specific degeneracy patterns

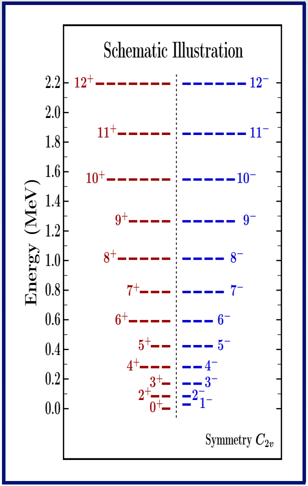

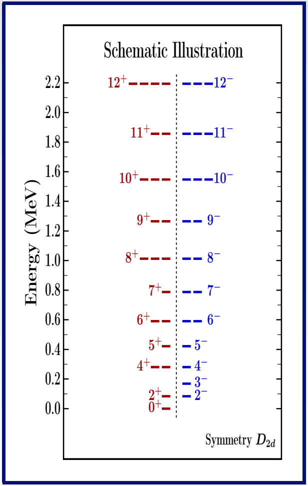

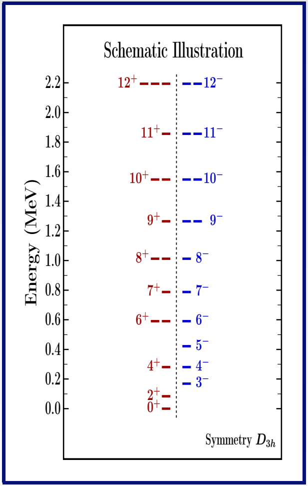

$\mathbf{C_{2v}}$: $(\alpha_{20}, \alpha_{31})$ $\mathbf{D_{2d}}$: $(\alpha_{20}, \alpha_{32})$ $\mathbf{D_{3h}}$: $(\alpha_{20}, \alpha_{33})$

Experimental Data Selection for C_{2v}

Experimental Data Selection for C_{2v}

- **Analysing NNDC experimental data for T_d symmetry in ^{152}Sm took 3 months of manual work**

Experimental Data Selection for C_{2v}

- **Analysing NNDC experimental data for T_d symmetry in ^{152}Sm**
  took 3 months of manual work

- **Collecting experimental evidence via NNDC for C_{2v} in ^{236}U**
  took 30 seconds of computer program*)

*) **I. Dedes in collaboration with M. Martin, Simon Fraser University, Canada**

Experimental Data Selection for C_{2v}

About criteria for the experimental data search

$C_{2v} \rightarrow A_1 : 0^+, 1^-, 2\times 2^+, 2^-, 3^+, 2\times 3^-, 3\times 4^+, 2\times 4^-, 2\times 5^+, 3\times 5^-, 4\times 6^+, 4\times 6^-, \cdots$

- Avoid rotational bands generated by leading ellipsoidal geometry and characterised by strong $\Delta I = 2$ quadrupole transitions
- Identified yrast-trap or K-isomers and related axial symmetry non-collective particle-hole excitations should be eliminated
- Energy-wise – C_{2v} bands form regular sequences

$$E_I \propto AI^2 + BI + C$$

Experimental Data Selection for C_{2v}

About criteria for the experimental data search

$$C_{2v} \rightarrow A_1 : 0^+,\ 1^-, 2\times 2^+, 2^-, 3^+, 2\times 3^-, 3\times 4^+, 2\times 4^-, 2\times 5^+, 3\times 5^-, 4\times 6^+, 4\times 6^-, \cdots$$

- Avoid rotational bands generated by leading ellipsoidal geometry and characterised by strong $\Delta I = 2$ quadrupole transitions
- Identified yrast-trap or K-isomers and related axial symmetry non-collective particle-hole excitations should be eliminated
- Energy-wise – C_{2v} bands form regular sequences

$$E_I \propto AI^2 + BI + C$$

Experimental Data Selection for C_{2v}

About criteria for the experimental data search

$C_{2v} \rightarrow A_1 : 0^+, 1^-, 2 \times 2^+, 2^-, 3^+, 2 \times 3^-, 3 \times 4^+, 2 \times 4^-, 2 \times 5^+, 3 \times 5^-, 4 \times 6^+, 4 \times 6^-, \cdots$

- Avoid rotational bands generated by leading ellipsoidal geometry and characterised by strong $\Delta I = 2$ quadrupole transitions
- Identified yrast-trap or K-isomers and related axial symmetry non-collective particle-hole excitations should be eliminated
- Energy-wise – $\mathbf{C_{2v}}$ bands form regular sequences

$$E_I \propto AI^2 + BI + C$$

Experimental Identification - Recent Results : ^{236}U

- Rotational band structure of a nucleus in a C_{2v}-symmetric configuration

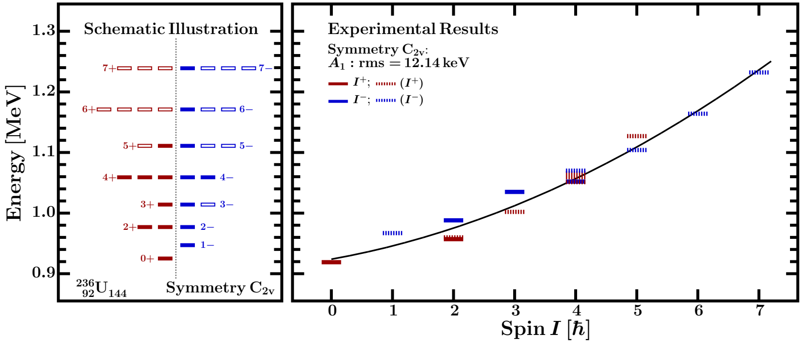

Attention: <u>Experimental</u> degeneracies for ^{236}U according to NNDC

Experimental Identification - Recent Results : ^{236}U

- Rotational band structure of a nucleus in a C_{2v}-symmetric configuration

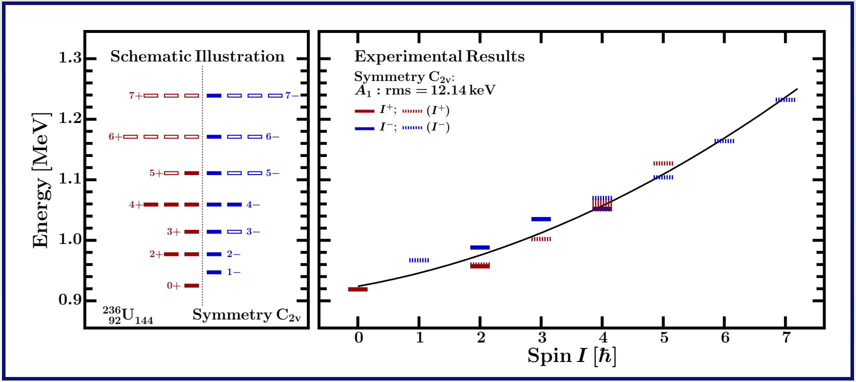

Attention: Experimental degeneracies for ^{236}U according to NNDC

- **Conclusion:**

1) Single rotational band followed by 16 states with rms deviation 12.14 keV

[rms(gsb)=3.79 keV]

Experimental Identification - Recent Results : ^{236}U

- **Rotational band of a nucleus in a C_{2v}-symmetric configuration**

Attention: Experimental degeneracies for ^{236}U according to NNDC

Experimental Identification - Recent Results : ^{236}U

- **Rotational band of a nucleus in a C_{2v}-symmetric configuration**

Attention: Experimental degeneracies for ^{236}U according to NNDC

- **Conclusions:**

1) Single rotational band followed by 16 states with rms deviation 12.14 keV

[rms(gsb)=3.79 keV]

Experimental Identification - Recent Results : ^{236}U

- **Rotational band of a nucleus in a C_{2v}-symmetric configuration**

Attention: Experimental degeneracies for ^{236}U according to NNDC

- **Conclusions:**

1) Single rotational band followed by 16 states with rms deviation 12.14 keV
[rms(gsb)=3.79 keV]

2) Degeneracies characteristic for C_{2v}-symmetry, even if partial, are there

Experimental Identification - Recent Results : ^{236}U

- **Rotational band of a nucleus in a C_{2v}-symmetric configuration**

Attention: Experimental degeneracies for ^{236}U according to NNDC

- **Conclusions:**

1) Single rotational band followed by 16 states with rms deviation 12.14 keV
[rms(gsb)=3.79 keV]

2) Degeneracies characteristic for C_{2v}-symmetry, even if partial, are there

3) The C_{2v} symmetry elements are:

- **E the identity operation**
- **C_2 a twofold symmetry axis**
- **σ_v the first mirror plane (xz)**
- **σ_v' the first mirror plane (yz)**

Experimental Identification - Recent Results : ^{236}U

- **Rotational band of a nucleus in a C_{2v}-symmetric configuration**

Attention: Experimental degeneracies for ^{236}U according to NNDC

- **Conclusions:**

1) Single rotational band followed by 16 states with rms deviation 12.14 keV
[rms(gsb)=3.79 keV]

2) Degeneracies characteristic for C_{2v}-symmetry, even if partial, are there

3) The C_{2v} symmetry elements are:

- E the identity operation
- C_2 a twofold symmetry axis
- σ_v the first mirror plane (xz)
- σ_v' the first mirror plane (yz)

- **H_2O has C_{2v}-symmetry:**

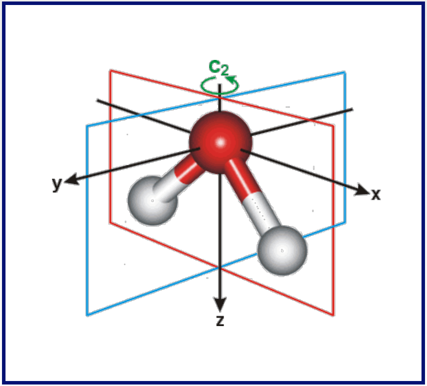

Exotic Symmetries for ^{236}U – Suspects for C_{2v}

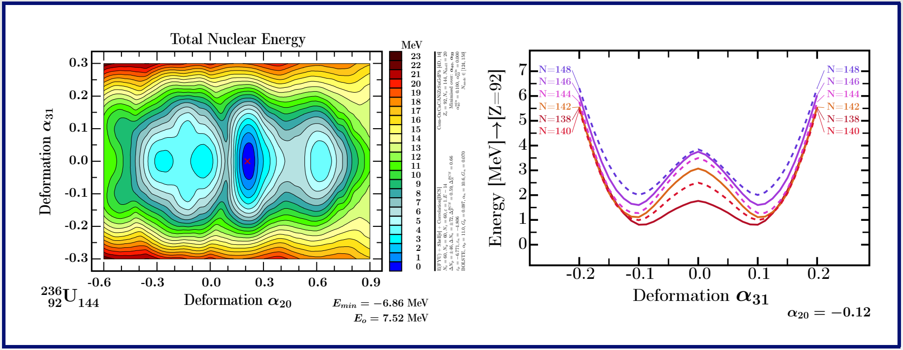

- We associate the prolate minimum at $\alpha_{20}^{th} \sim 0.25$ [r.m.s.$(\alpha_{20}^{exp}) = 0.2821(18)$]$^{*)}$ with the ground-state,...

- ... and the oblate minimum at $\alpha_{20}^{th} \sim -0.12$ extended on α_{31} as the C_{2v} symmetry

$^{*)}$ S. Raman, C. W. Nestor, JR., and P. Tikkanen
Atomic Data and Nuclear Data Tables, Vol. 78, No. 1, May 2001

We know that the potential energy landscapes may only give qualitative suggestions about equilibrium deformations → shapes & symmetries

We know that the potential energy landscapes may only give qualitative suggestions about equilibrium deformations → shapes & symmetries

We will turn to the s o l u t i o n s of the collective Schrödinger equation!!

Collective Schrödinger Equation

• Our group has developed*) new concepts of adiabaticity within collective model of Bohr and related approach to collective inertia tensor

• Using a newly re-formulated concept of adiabaticity and perturbation theory a new method of calculating collective inertia tensor $B_{\alpha_{\lambda,\mu},\alpha_{\lambda',\mu'}}(\alpha)$ is obtained

• The new expression is free form destructive divergencies contained in all the preceding formulations of this theory ← Particularly important new result

• Collective excitations in ^{208}Pb are reproduced without parameter adjustments

Collective Schrödinger Equation

• Our group has developed*) new concepts of adiabaticity within collective model of Bohr and related approach to collective inertia tensor

• Using a newly re-formulated concept of adiabaticity and perturbation theory a new method of calculating collective inertia tensor $B_{\alpha_{\lambda,\mu},\alpha_{\lambda',\mu'}}(\alpha)$ is obtained

• The new expression is free form destructive divergencies contained in all the preceding formulations of this theory ← Particularly important new result

• Collective excitations in ^{208}Pb are reproduced without parameter adjustments

• All the details, illustrations, comparisons with experiment can be found in:

"A New Approach to Adiabaticity Concepts in Collective Nuclear Motion: Impact for the Collective-Inertia Tensor and Comparisons with Experiment"

*) PHYSICAL REVIEW C 99, 041303(R) (2019)

D. Rouvel and J. Dudek

Collective Schrödinger Equation

- It follows that the collective energy operator is ($q^m \leftrightarrow \alpha_{\lambda,\mu}$, B-mass tensor)

$$\hat{H}_{\rm coll} = -\frac{\hbar^2}{2}\Delta + V(\alpha) \;\leftrightarrow\; \Delta \stackrel{df.}{=} \sum_{m,n=1}^{d} \frac{1}{\sqrt{|B|}} \frac{\partial}{\partial q^n}\left(\sqrt{|B|} B^{nm} \frac{\partial}{\partial q^m}\right).$$

with the resulting collective Schrödinger equation

$$\boxed{\hat{H}_{\rm coll}\Psi_{\rm coll} = E_{\rm coll}\Psi_{\rm coll}}$$

Collective Schrödinger Equation

- It follows that the collective energy operator is ($q^m \leftrightarrow \alpha_{\lambda,\mu}$, B-mass tensor)

$$\hat{H}_{\text{coll}} = -\frac{\hbar^2}{2}\Delta + V(\alpha) \;\leftrightarrow\; \Delta \stackrel{df.}{=} \sum_{m,n=1}^{d} \frac{1}{\sqrt{|B|}} \frac{\partial}{\partial q^n} \left(\sqrt{|B|} B^{nm} \frac{\partial}{\partial q^m} \right).$$

with the resulting collective Schrödinger equation

$$\boxed{\hat{H}_{\text{coll}} \Psi_{\text{coll}} = E_{\text{coll}} \Psi_{\text{coll}}}$$

- All the details, illustrations, comparisons with experiment can be found in:

A New Approach to Adiabaticity Concepts in Collective Nuclear Motion: Impact for the Collective-Inertia Tensor and Comparisons with Experiment

PHYSICAL REVIEW C 99, 041303(R) (2019)

D. Rouvel and J. Dudek

Collective Schrödinger Equation for C_{2v}

- The most probable α_{31} deformation $\leftrightarrow$ the so-called "dynamic equilibrium" $\leftrightarrow$ the most probable C_{2v}-symmetric shape

$$\alpha_{31}^{\text{dyn}} \;\leftrightarrow\; \langle \alpha_{31}^2 \rangle = \int \Psi^*(\alpha_{31})\alpha_{31}^2 \Psi(\alpha_{31}) d\alpha_{31}$$

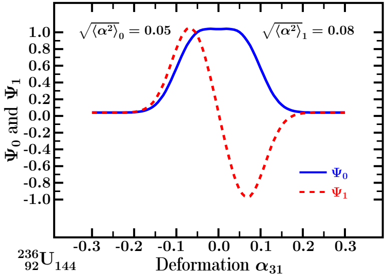

- Resulting dynamical equilibrium values are close to typical values of the secondary deformations such as the hexadecapole one reported in many nuclei

Summary and Conclusions

Background and Motivation of this Project

• Using the newest exp. results, we adjusted the 12 universal WS parameters common for the whole mass table employing the Inverse Problem Theory of applied mathematics to assure prediction stability especially for exotic nuclei

Summary and Conclusions

Background and Motivation of this Project

• Using the newest exp. results, we adjusted the 12 universal WS parameters common for the whole mass table employing the Inverse Problem Theory of applied mathematics to assure prediction stability especially for exotic nuclei

• We have performed large-scale nuclear potential-energy calculations in multidimensional $\alpha_{\lambda,\mu}$-deformation spaces – for over 700 even-even nuclei →

Here we illustrated exotic symmetry effects near ^{208}Pb

Summary and Conclusions

Background and Motivation of this Project

• Using the newest exp. results, we adjusted the 12 universal WS parameters common for the whole mass table employing the Inverse Problem Theory of applied mathematics to assure prediction stability especially for exotic nuclei

• We have performed large-scale nuclear potential-energy calculations in multidimensional $\alpha_{\lambda,\mu}$-deformation spaces – for over 700 even-even nuclei → Here we illustrated exotic symmetry effects near ^{208}Pb

• We focussed attention on a universal magic gap $N = 136$ generating strong shell effects/minima for α_{30}, α_{31}, α_{32} and α_{33} deformations – simultaneously

Summary and Conclusions

Background and Motivation of this Project

• Using the newest exp. results, we adjusted the 12 universal WS parameters common for the whole mass table employing the Inverse Problem Theory of applied mathematics to assure prediction stability especially for exotic nuclei

• We have performed large-scale nuclear potential-energy calculations in multidimensional $\alpha_{\lambda,\mu}$-deformation spaces – for over 700 even-even nuclei → Here we illustrated exotic symmetry effects near ^{208}Pb

• We focussed attention on a universal magic gap $N = 136$ generating strong shell effects/minima for α_{30}, α_{31}, α_{32} and α_{33} deformations – simultaneously

• We applied the standard group-, and point-group theory as tools to predict rotational band spin-parity sequences – to identify the new exotic symmetries

Summary and Conclusions

Background and Motivation of this Project

• Using the newest exp. results, we adjusted the 12 universal WS parameters common for the whole mass table employing the Inverse Problem Theory of applied mathematics to assure prediction stability especially for exotic nuclei

• We have performed large-scale nuclear potential-energy calculations in multidimensional $\alpha_{\lambda,\mu}$-deformation spaces – for over 700 even-even nuclei → Here we illustrated exotic symmetry effects near ^{208}Pb

• We focussed attention on a universal magic gap $N = 136$ generating strong shell effects/minima for α_{30}, α_{31}, α_{32} and α_{33} deformations – simultaneously

• We applied the standard group-, and point-group theory as tools to predict rotational band spin-parity sequences – to identify the new exotic symmetries

• Should stable minima or dynamical equilibrium deformations appear as associated with either α_{30} or α_{31} or α_{32} or α_{33} deformations, they would generate point group symmetries $C_{\infty v}$, C_{2v}, T_d and D_{3h}

Summary and Conclusions

Background and Motivation of this Project

• Using the newest exp. results, we adjusted the 12 universal WS parameters common for the whole mass table employing the Inverse Problem Theory of applied mathematics to assure prediction stability especially for exotic nuclei

• We have performed large-scale nuclear potential-energy calculations in multidimensional $\alpha_{\lambda,\mu}$-deformation spaces – for over 700 even-even nuclei $\rightarrow$ Here we illustrated exotic symmetry effects near ^{208}Pb

• We focussed attention on a universal magic gap $N = 136$ generating strong shell effects/minima for α_{30}, α_{31}, α_{32} and α_{33} deformations – simultaneously

• We applied the standard group-, and point-group theory as tools to predict rotational band spin-parity sequences – to identify the new exotic symmetries

• Should stable minima or dynamical equilibrium deformations appear as associated with either α_{30} or α_{31} or α_{32} or α_{33} deformations, they would generate point group symmetries $C_{\infty v}$, C_{2v}, T_d and D_{3h}

• We have presented to our knowledge the world first identification of the exotic C_{2v} point group symmetry – a confirmation of the symmetry approach

This presentation is based on the theory methods illustrated in the recent articles:

Spectroscopic criteria for identification of nuclear tetrahedral and octahedral symmetries: Illustration on a Rare Earth nucleus

PHYSICAL REVIEW C 97, 021302(R) (2018)

J. Dudek, D. Curien, I. Dedes, K. Mazurek, S. Tagami, Y. R. Shimizu and T. Bhattacharjee

Predictive Power of theoretical modelling of the nuclear mean field: Examples of improving predictive capacities

PHYSICA SCRIPTA 93, 044003 (2018)

I. Dedes, and J. Dudek

Propagation of the nuclear mean-field uncertainties with increasing distance from the parameter adjustment zone: Applications to superheavy nuclei

PHYSICAL REVIEW C 99, 054310 (2019)

I. Dedes, and J. Dudek

Exotic shape symmetries around the fourfold octupole magic number $N = 136$: Formulation of experimental identification criteria

PHYSICAL REVIEW C 105, 034348 (2022)

J. Yang, J. Dudek, I. Dedes, A. Baran, D. Curien, A. Gaamouci, A. Góźdź, A. Pędrak, D. Rouvel, H. L. Wang, and J. Burkat